Microwave-Assisted Dehydrogenation of Fossil Fuels Using Iron-Based Alumina Nanocomposites

Award No.: DE-FE0032086
Award Recipient: The University of Texas at El Paso
Principal Investigator: Evgeny Shafirovich
Graduate Research Assistants: Zachary A. Chanoi (PhD Student)
Laura A. Martinez (M.S. student)
Victoria I. Reyes (M.S. student)
Program Manager: Maria M. Reidpath (retired),
Alison E. Metz
Period of Performance: 8/15/2021 – 8/14/2024
Pending NCE to 1/15/2025
Amount: $400K

The Students

Victoria Reyes

- Graduated with M.S. in 2022, with a thesis on the synthesis of Fe/SiC.

Laura Martinez

- M.S. student studying thermogravimetric analysis of $FeAl_xO_y$ combustion synthesis.

Zachary Chanoi

- Ph.D. student studying microwave-assisted production of H_2 from hydrocarbons.

Together we have accomplished:

1 M.S. Thesis

1 journal article published, 1 under review

8 conference presentations

Peer-reviewed Journal Articles:

"Dielectric and magnetic properties of microwave-absorbing $FeAl_xO_y$ fabricated via solution combustion synthesis," *Ceramics International,* (2024), Under-review.

"Toward a tunable fabrication of multifunctional iron-aluminum spinels via solution combustion synthesis: The effects of fuel, heating mode, and Fe:Al precursor ratio," *Ceramics International* 49 (2023) 39049-39058.

Theses/Dissertations:

Reyes, V.I., "Fabrication and characterization of iron-based catalysts for the dehydrogenation of fossil fuels," M.S. Thesis, The University of Texas at El Paso, 2022.

Presentations:

2023 AIChE Annual Meeting, Nov. 5-10, 2023, Orlando, FL.

2023 FECM/NETL Spring R&D Project Review Meeting, April 17-20, 2023, Pittsburgh, PA (*honorable mention of student presentation*).

13th U. S. National Combustion Meeting Organized by the Central States Section of the Combustion Institute, March 19-22, 2023, College Station, TX.

2022 AIChE Annual Meeting, Nov. 13-18, 2022, Phoenix, AZ.

2022 Spring Technical Meeting of the Central States Section of The Combustion Institute, May 15-17, 2022, Detroit, MI, Paper 2B04 (*First Place for Technical Merit in the Combustion Art Competition*).

Student Conferences:

2024 Southwest Emerging Technology Symposium, April 17-18, 2024, El Paso, TX.

2023 Southwest Emerging Technology Symposium, April 24-25, 2023, El Paso, TX.

2022 Southwest Emerging Technology Symposium, April 12-13, 2022, El Paso, TX.

Where this project has taken us

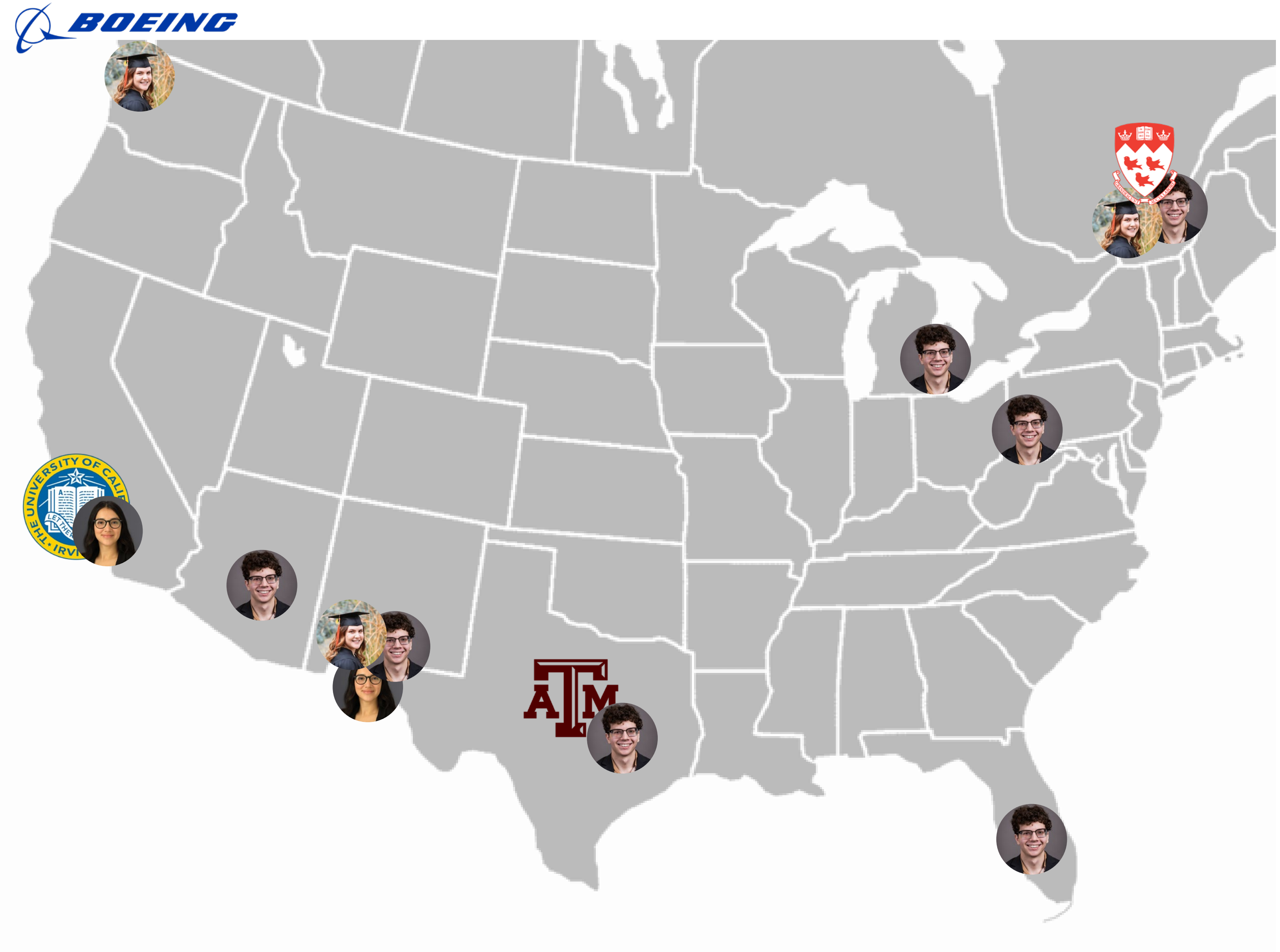

The Students

We **need** hydrogen for:

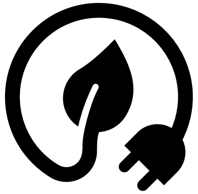

Clean energy carrier

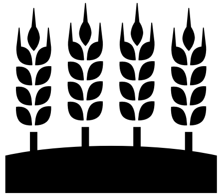

Agriculture

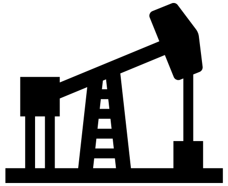

Refining

- The demand for hydrogen is increasing dramatically – from **120 Mt** (2020) to a projected **530 Mt** (2050) [1].

- Hydrogen (H_2) is necessary for developing clean energy technologies and many other important applications. **95%** of H_2 comes from fossil fuel.

- Steam reforming of methane (CH_4) is the main method for H_2 production, but it also produces lots of CO_2.
  - 8.5 – 10 kg of CO_2 per 1 kg of H_2

[1] Hermesmann et al. 2022. *Progress in Energy and Combustion Science*

Using microwaves to split fossil fuels

- Microwave-assisted, thermocatalytic, dehydration of fossil fuels offers the potential to produce H_2 without CO_2.
- Carbon is stored as valuable carbon nanotubes (CNT).
- Need a material that is both catalytically active and a good microwave-absorber.

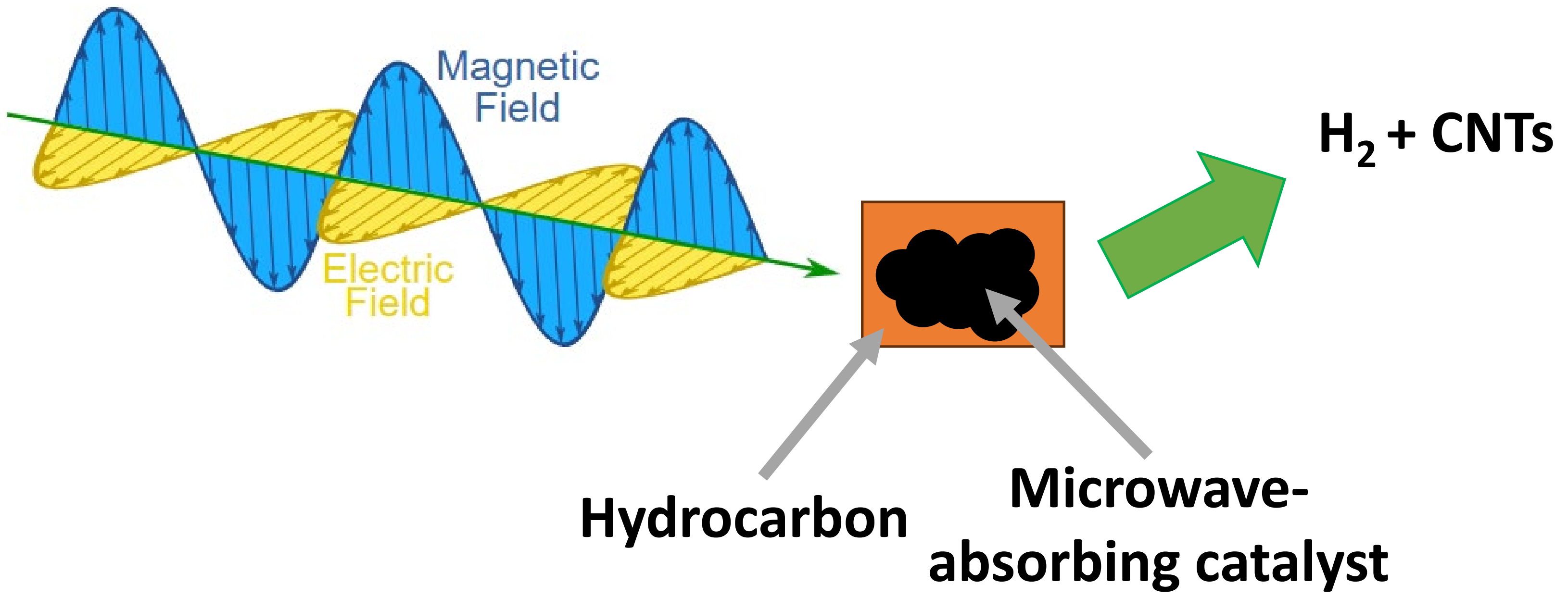

Why microwaves?

- Microwaves enable instantaneous and volumetric heating of materials.

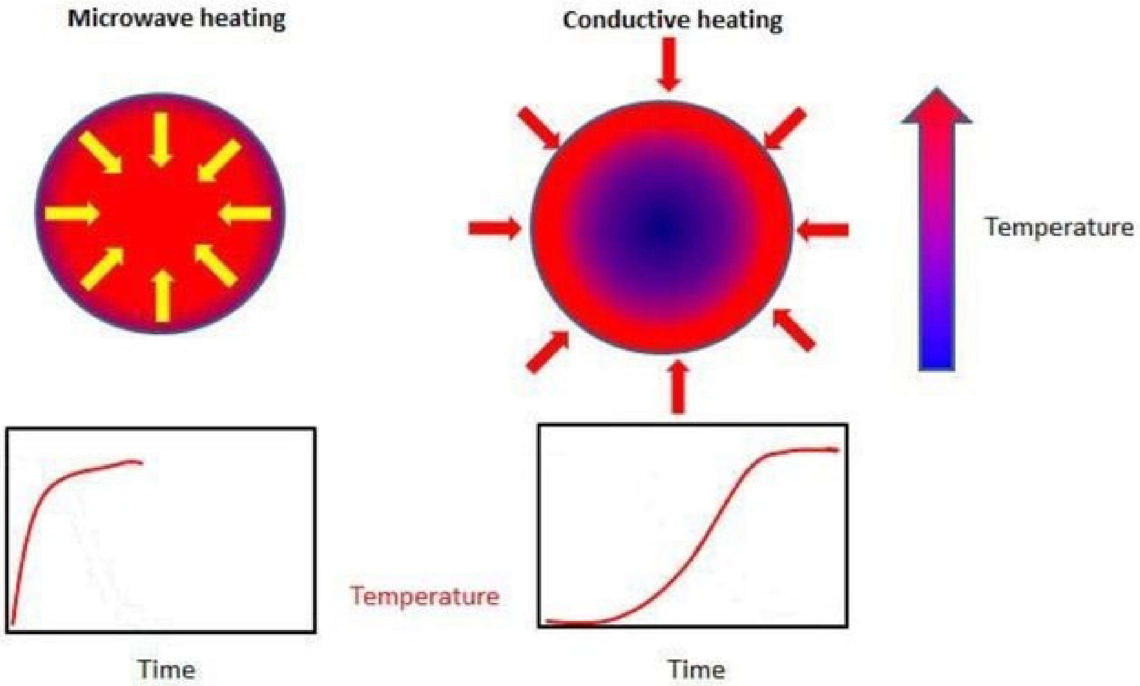

[2] Palma et al. 2020. *Catalysis*.

- Improves energy efficiency and selectivity of reactions.

Why microwaves?

Microwave | Conventional furnace

CH_4 conversion

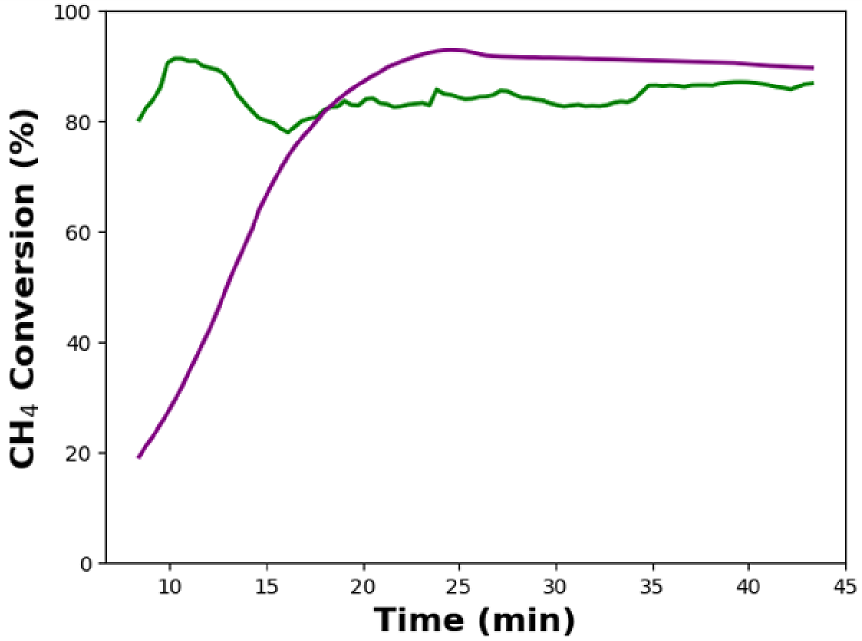

The microwave's **instant heating** led to higher conversions sooner.

Energy efficiency

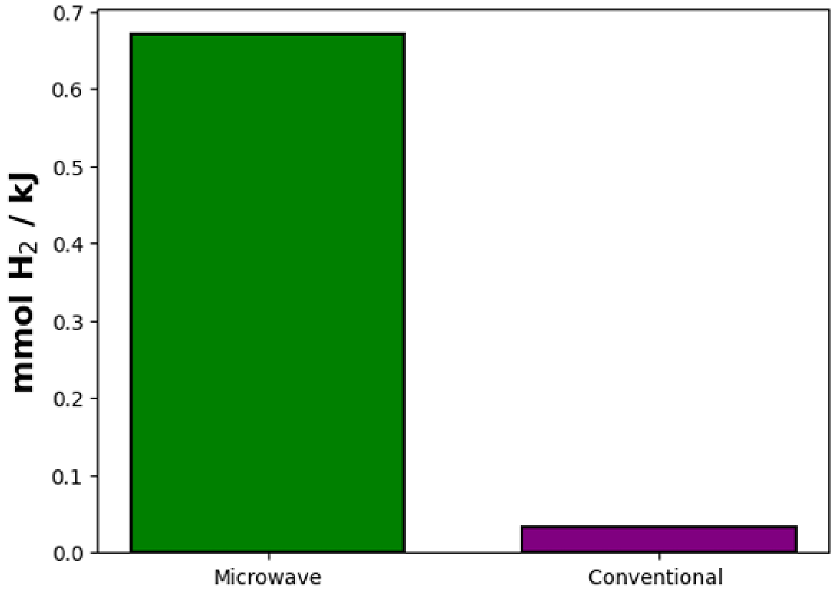

More H2 produced per unit of energy spent.

Solution combustion synthesis (SCS)

- Technique for fabrication of nanomaterials
    - Rapid and simple
    - Energy efficient and scalable [3]
    - Large design space enabled by many synthesis parameters

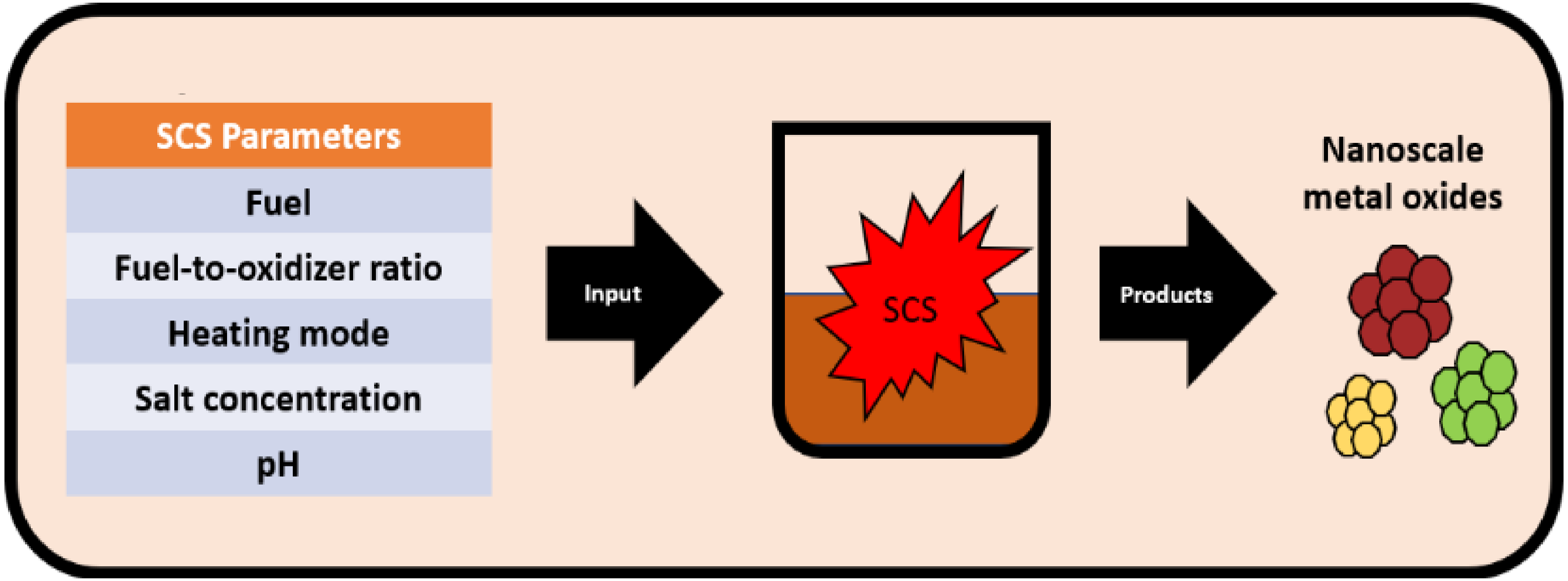

[3] Li et al. 2015. *Nanoscale.*

Overview

Tunable catalyst combustion synthesis:

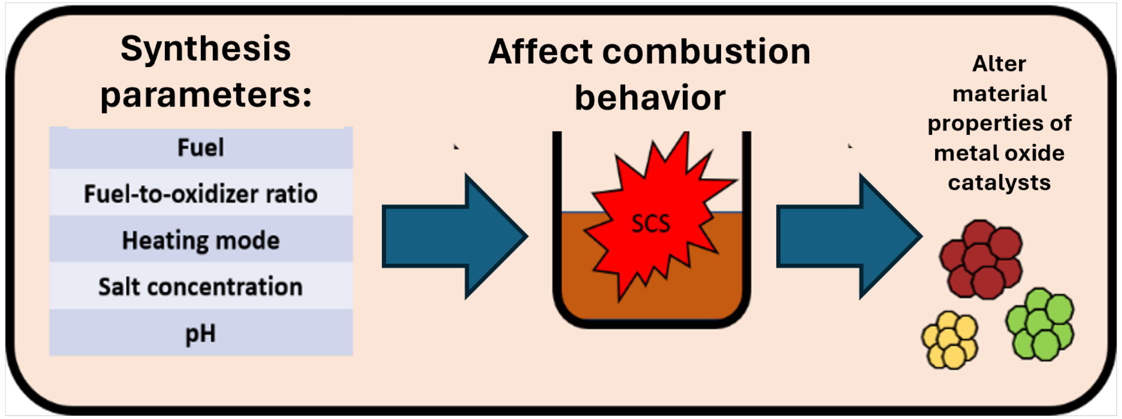

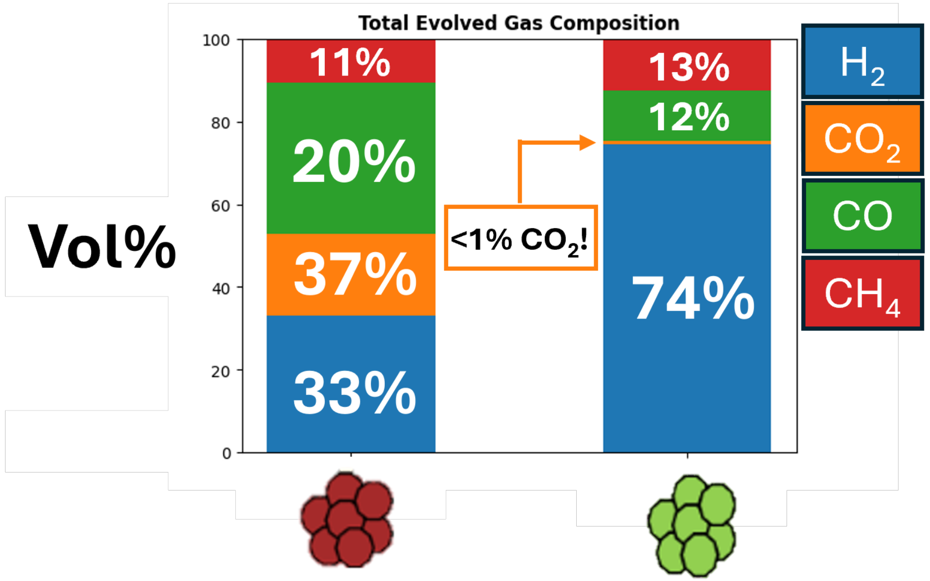

Subtle changes induce statistically significant differences:

Catalysts are catalytically active and excellent microwave absorbers:

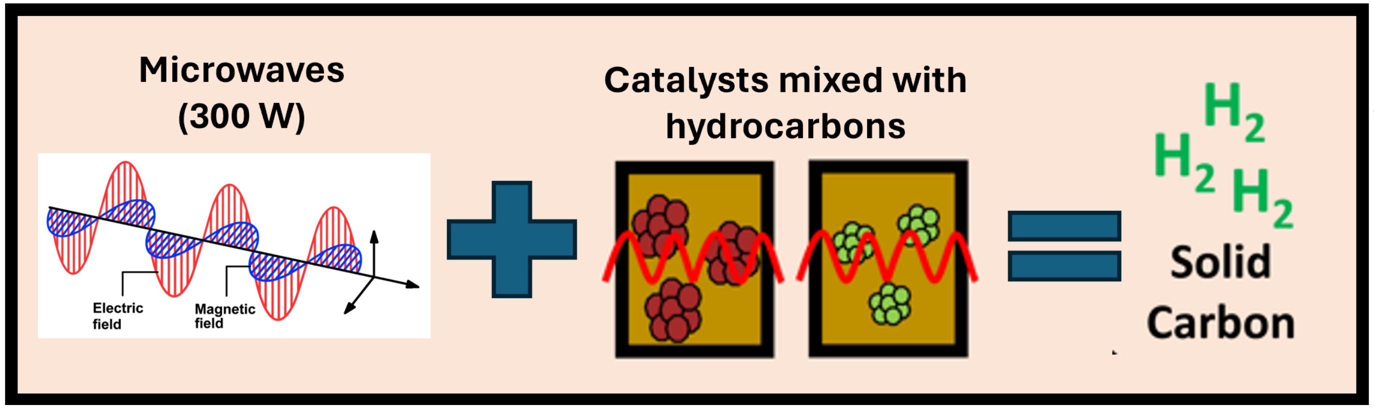

Objectives

Objectives

1. To determine optimal parameters of **solution combustion synthesis** for the fabrication of **iron-based alumina nanocomposites** with superior catalytic activity, microwave absorptivity, and ferrimagnetic properties.

2. To determine the effectiveness of the iron-based alumina nanocomposites in the microwave-assisted catalytic decomposition of crude oil, diesel fuel, and gasoline in terms of hydrogen selectivity and yield.

3. To investigate regeneration of the iron-based alumina nanocomposites by microwave-assisted gasification of the formed carbon and by magnetic separation of the catalyst particles from the carbon byproducts.

Abbreviated objectives

Objectives

1. Optimize catalyst **production** via solution combustion synthesis.
2. Optimize catalyst **properties** during microwave-assisted dehydrogenation.
3. Optimize catalyst **sustainability** post-dehydrogenation.

Timeline and milestones

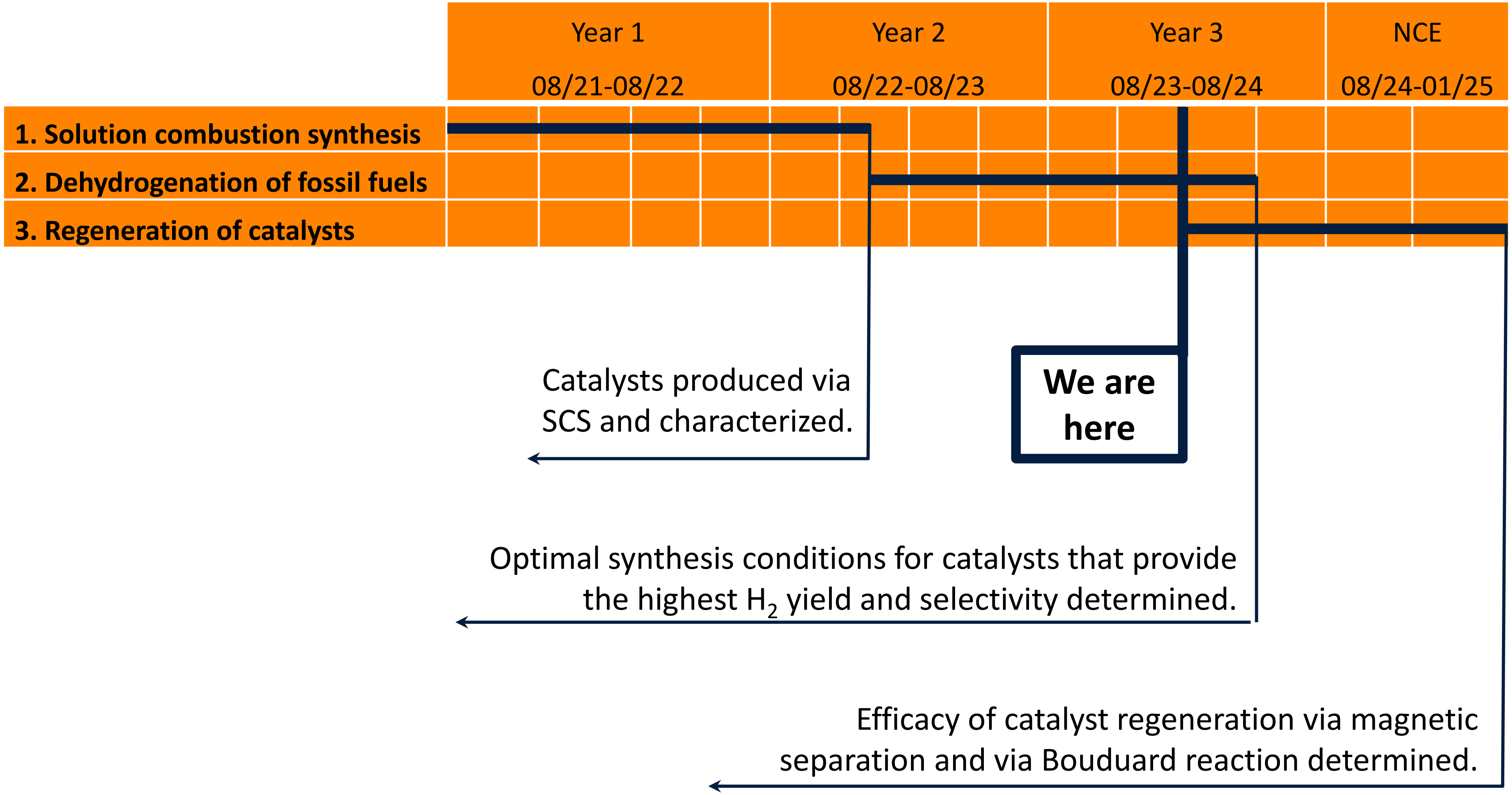

Methodology

Objective 1

1. Fuel: glycine (**G**) vs. citric acid (**CA**)
2. Heating mode: furnace (**F**) vs. hotplate (**H**)
3. Fe/Al ratio: iron-lean (**1:2**), balanced (**1:1**), and iron-rich (**2:1**)

	1:2	**1:1**	**2:1**
		Citric Acid	
Hotplate	1:2-CA-H	1:1-CA-H	2:1-CA-H
Furnace	1:2-CA-F	1:1-CA-F	2:1-CA-F
		Glycine	
Hotplate	1:2-G-H	1:1-G-H	2:1-G-H
Furnace	1:2-G-F	1:1-G-F	2:1-G-F

Objective 1

Glycine combustion

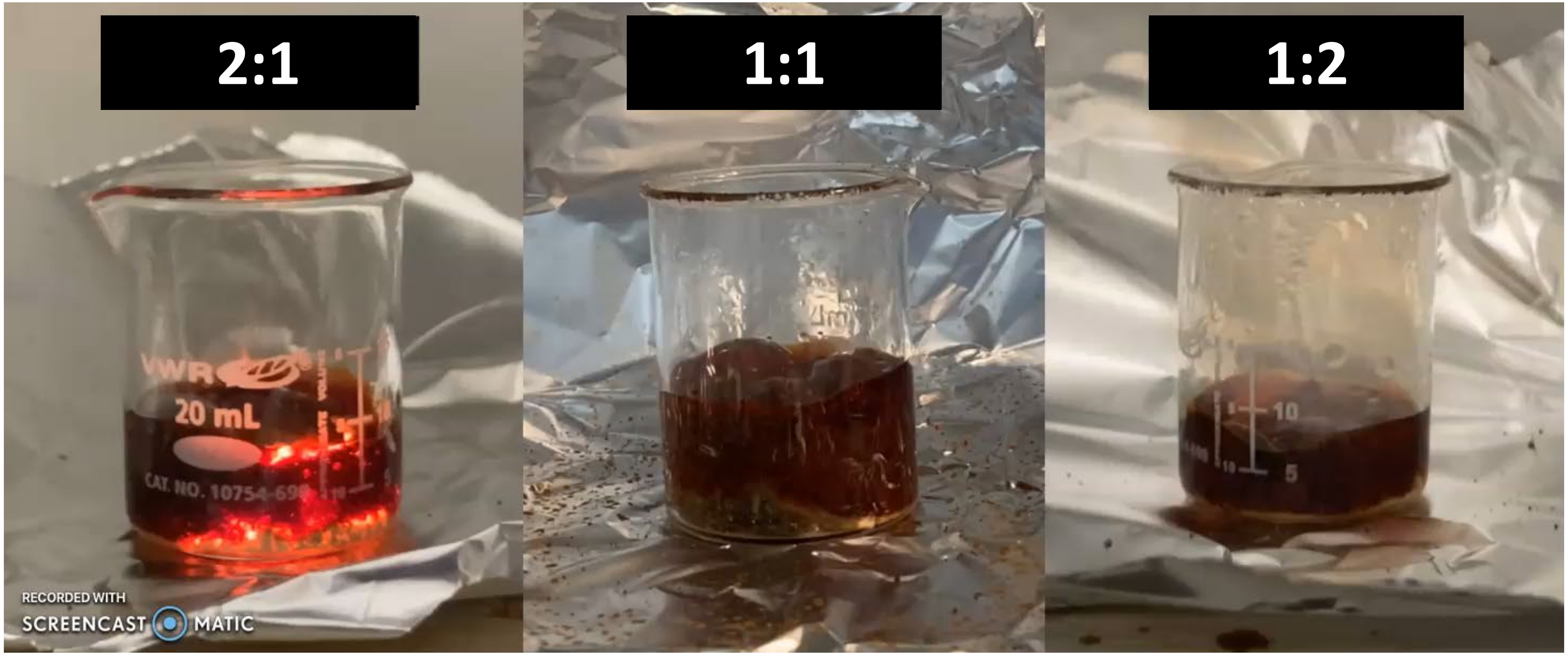

- Solid-phase formation lasted about 10 seconds.
- Visible flame depending on the Fe:Al molar ratio.

Differences between combustion heating mode

Furnace

VS.

Hotplate

- For glycine, products synthesized in the furnace were more homogenous of color, while products made on the hotplate had more dendritic structure.

Objective 1

Morphology

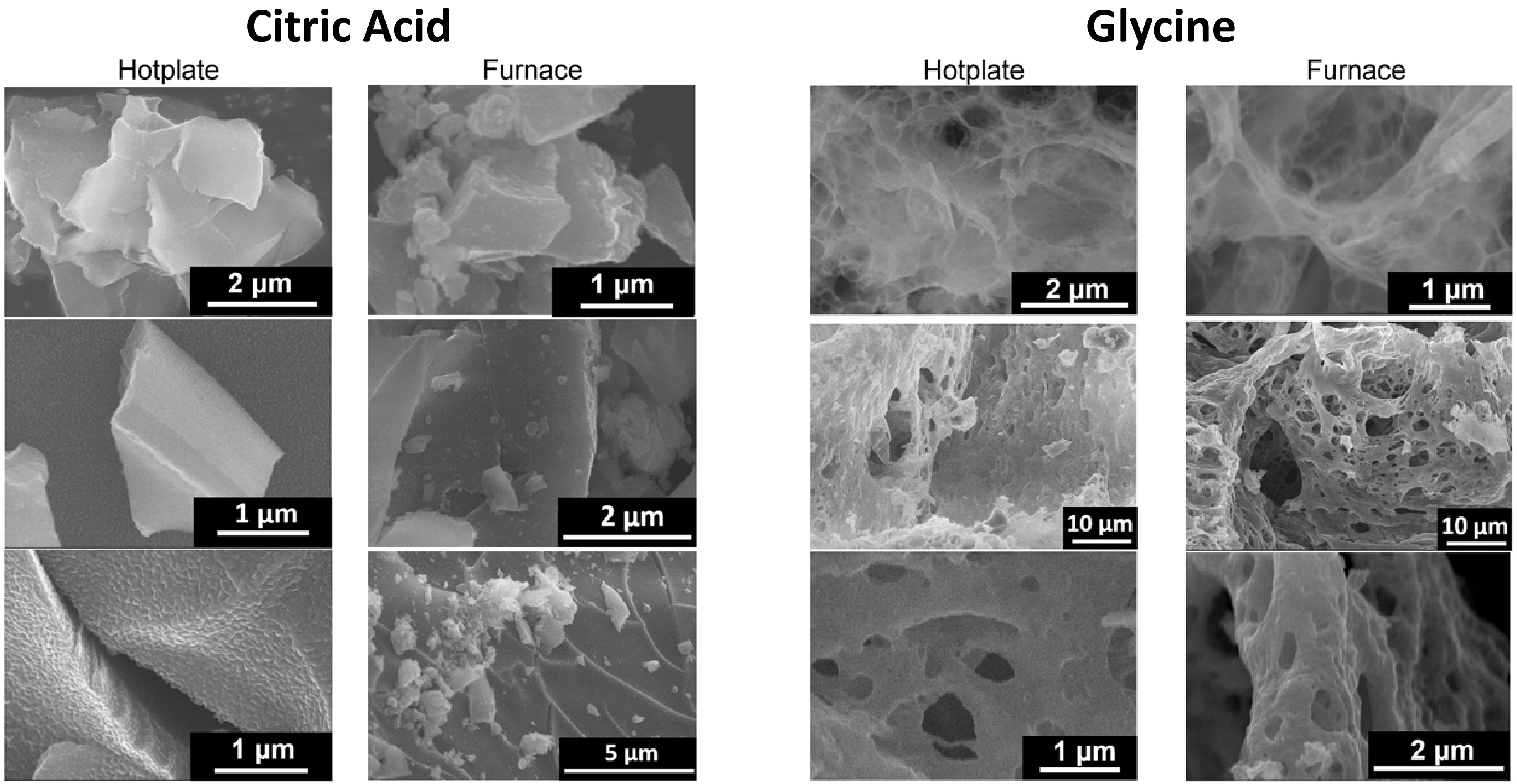

- Glycine products had an abundance of micropores.
- Citric acid products were characterized by thin flake-like structures.

Objective 1

X-Ray diffraction

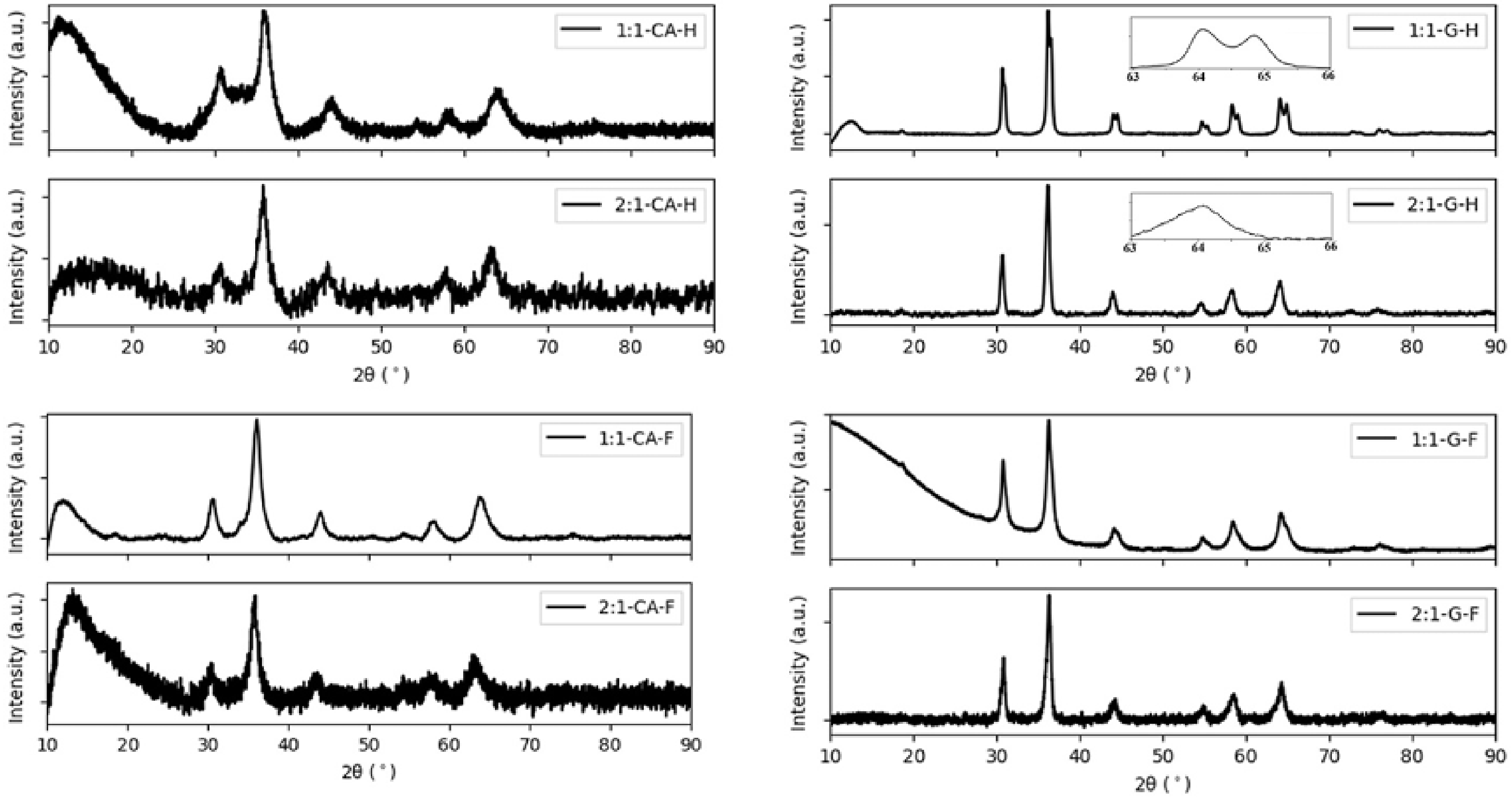

- For all products except Fe:Al molar ratio 1:2, the typical diffraction pattern for spinels was observed (F$\bar{d}$3m).
- CA-derived catalysts had γ-Fe_2O_3 structure, while G-derived catalysts had $FeAl_2O_4$-Fe_3O_4 structure.

BET specific surface area

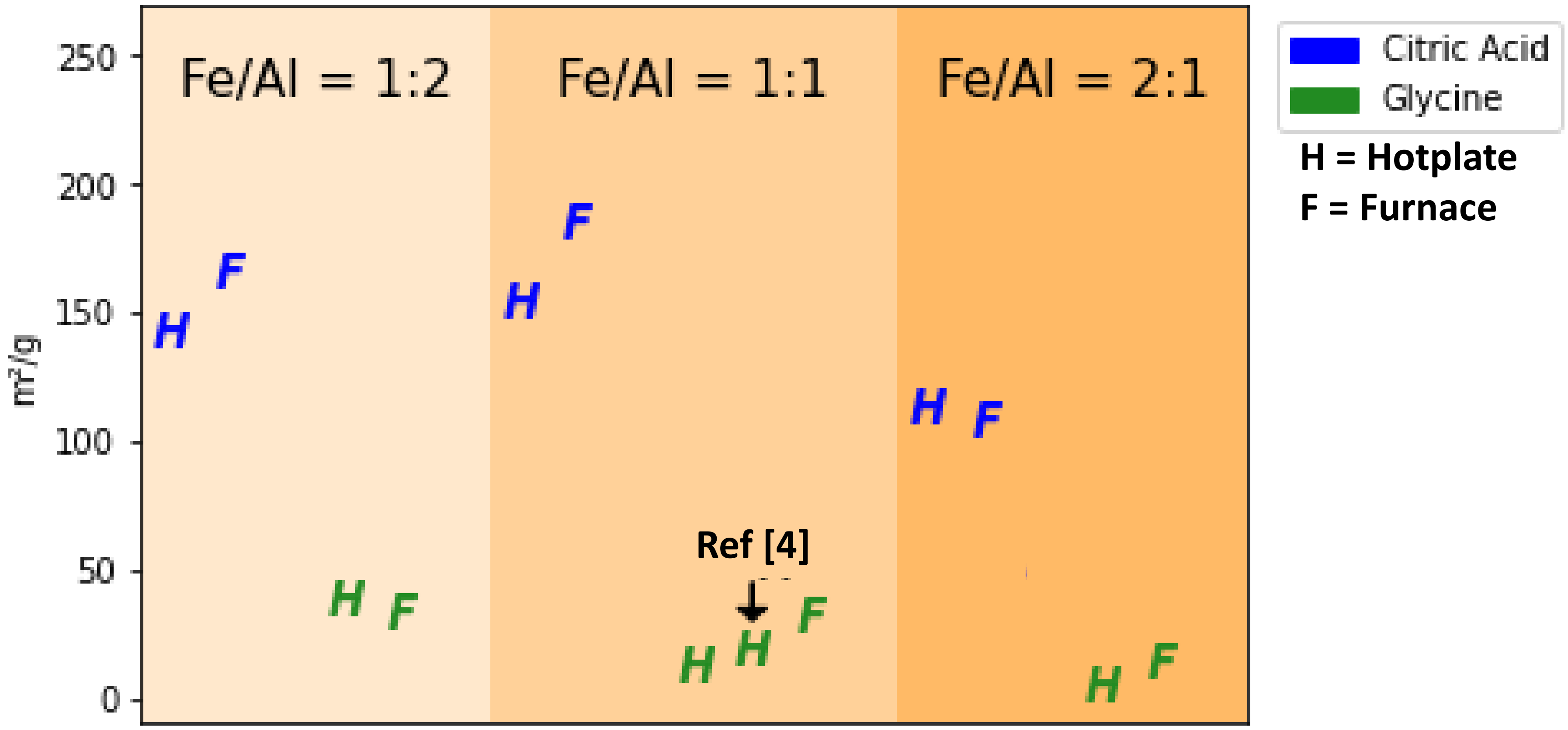

- High specific surface area achieved
- Strongly dependent on fuel and heating mode

[4] Pehlivan et al. *Journal of Materials Research and Technology* 8, (2019).

Microwave heating performance

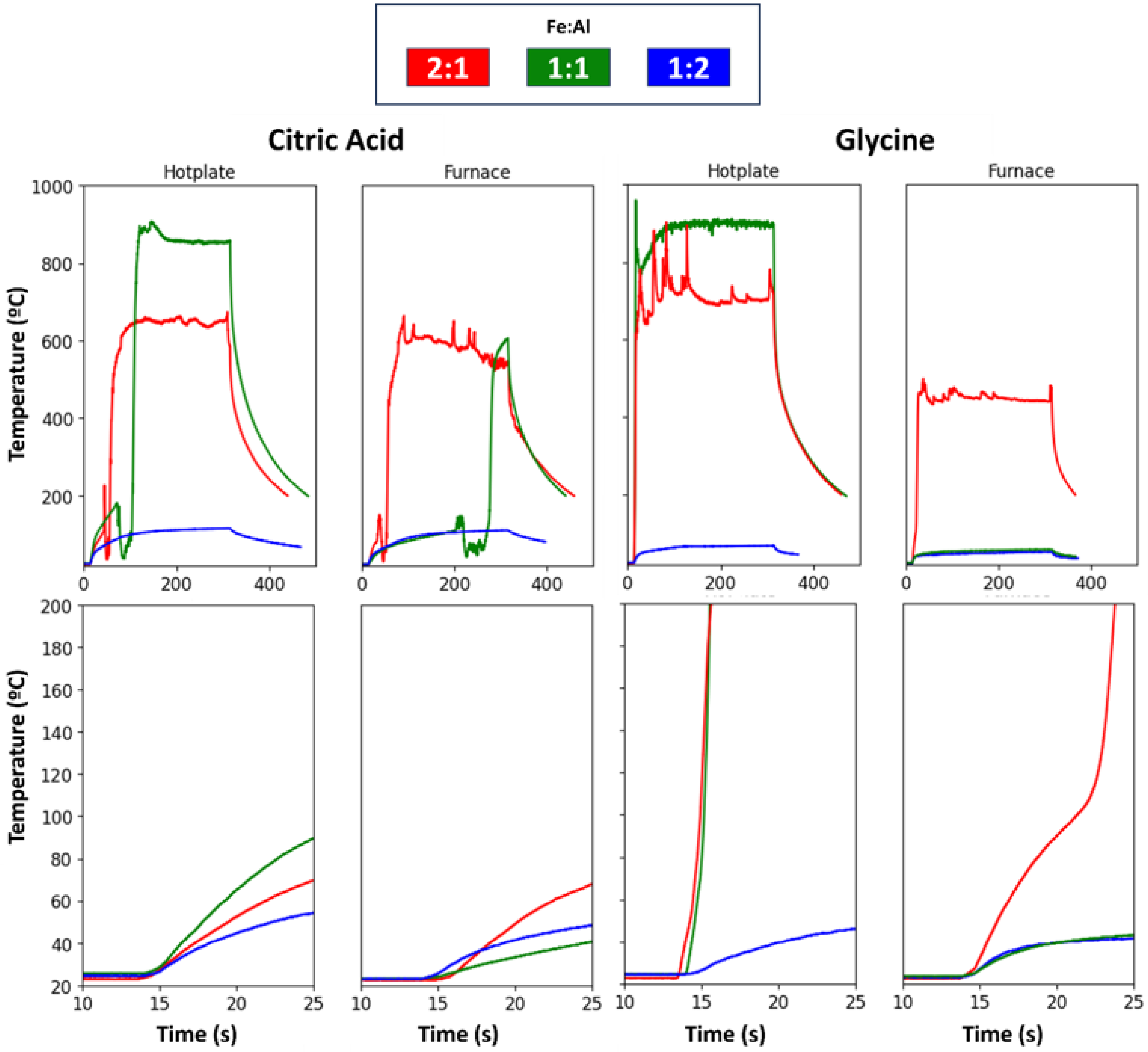

Initial heating

- Initial heating rate was higher for G-derived catalysts.
- 1:1-G-F had remarkably low heating rate compared to other products due to lower penetration depth.

Setup for microwave-assisted dehydrogenation

IR Pyrometer

Quartz reactor

Microwave

Cold trap

Gas sample bag

GC

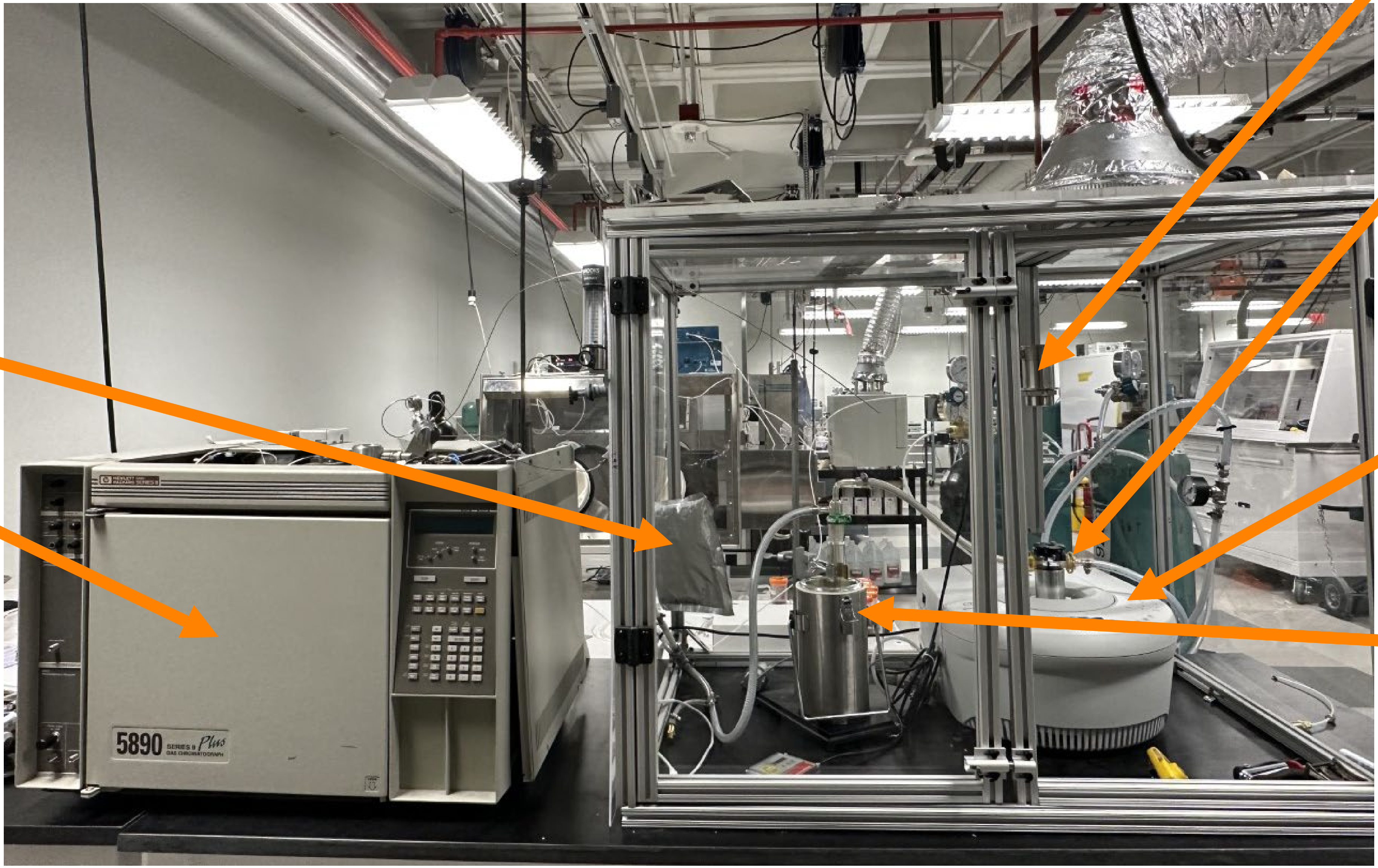

Dehydrogenation procedure

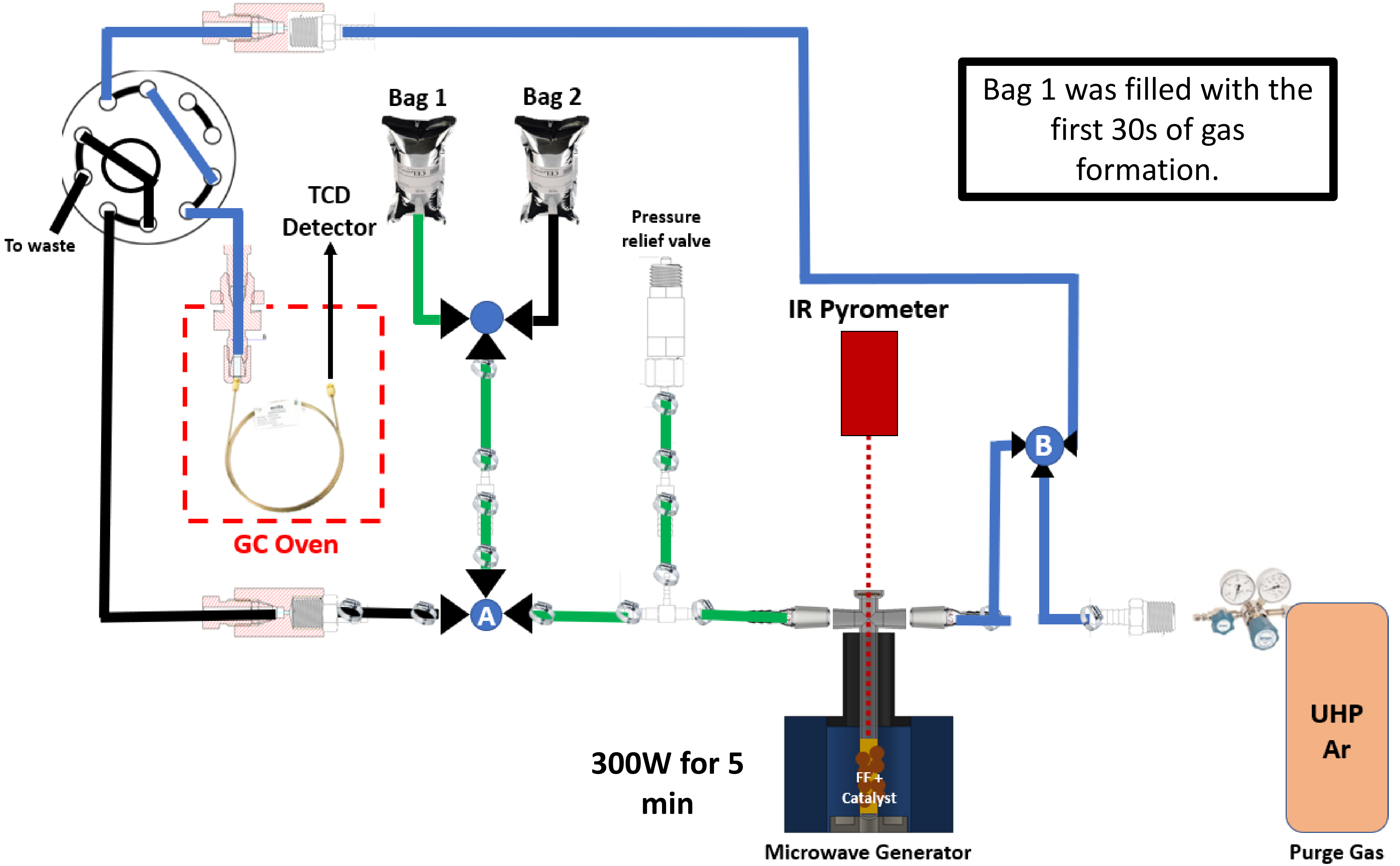

Bag 1 was filled with the first 30s of gas formation.

300W for 5 min

Dehydrogenation procedure

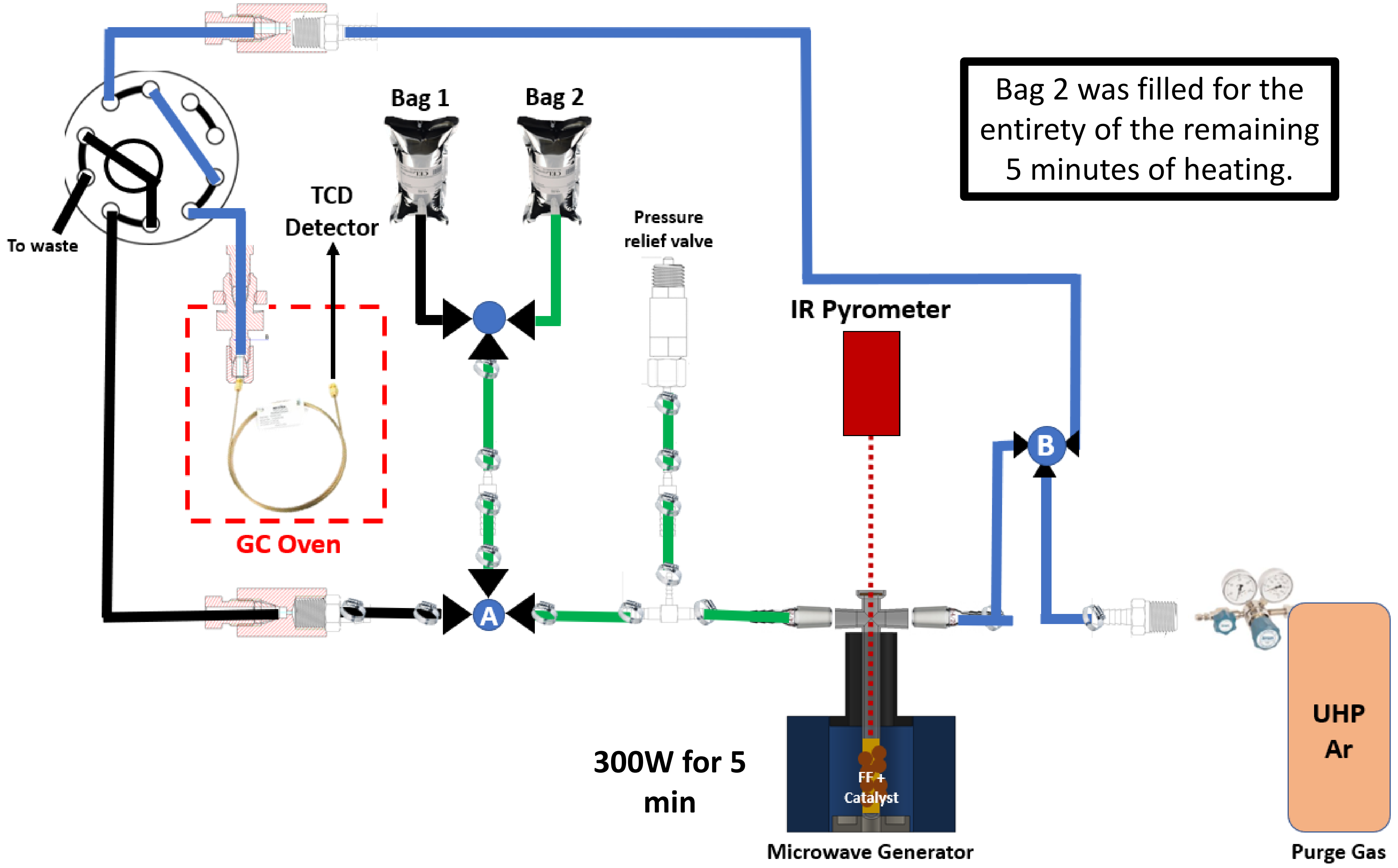

Bag 2 was filled for the entirety of the remaining 5 minutes of heating.

300W for 5 min

Objective 2

Dehydrogenation procedure

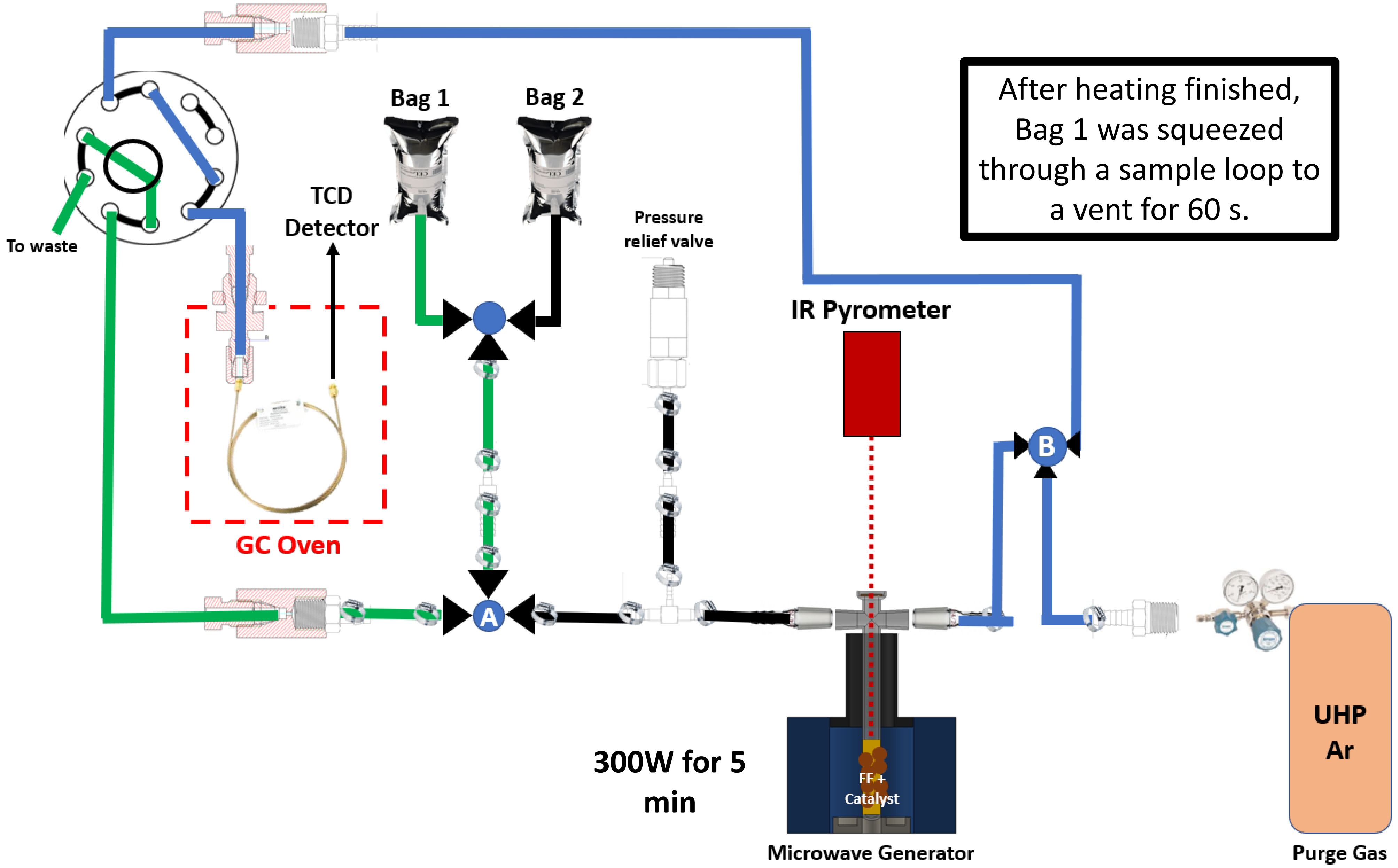

After heating finished, Bag 1 was squeezed through a sample loop to a vent for 60 s.

Dehydrogenation procedure

The valve was then switched to mix the carrier gas with the filled sample loop, injecting the gas mixture onto the GC column.

This process was repeated for Bag 2.

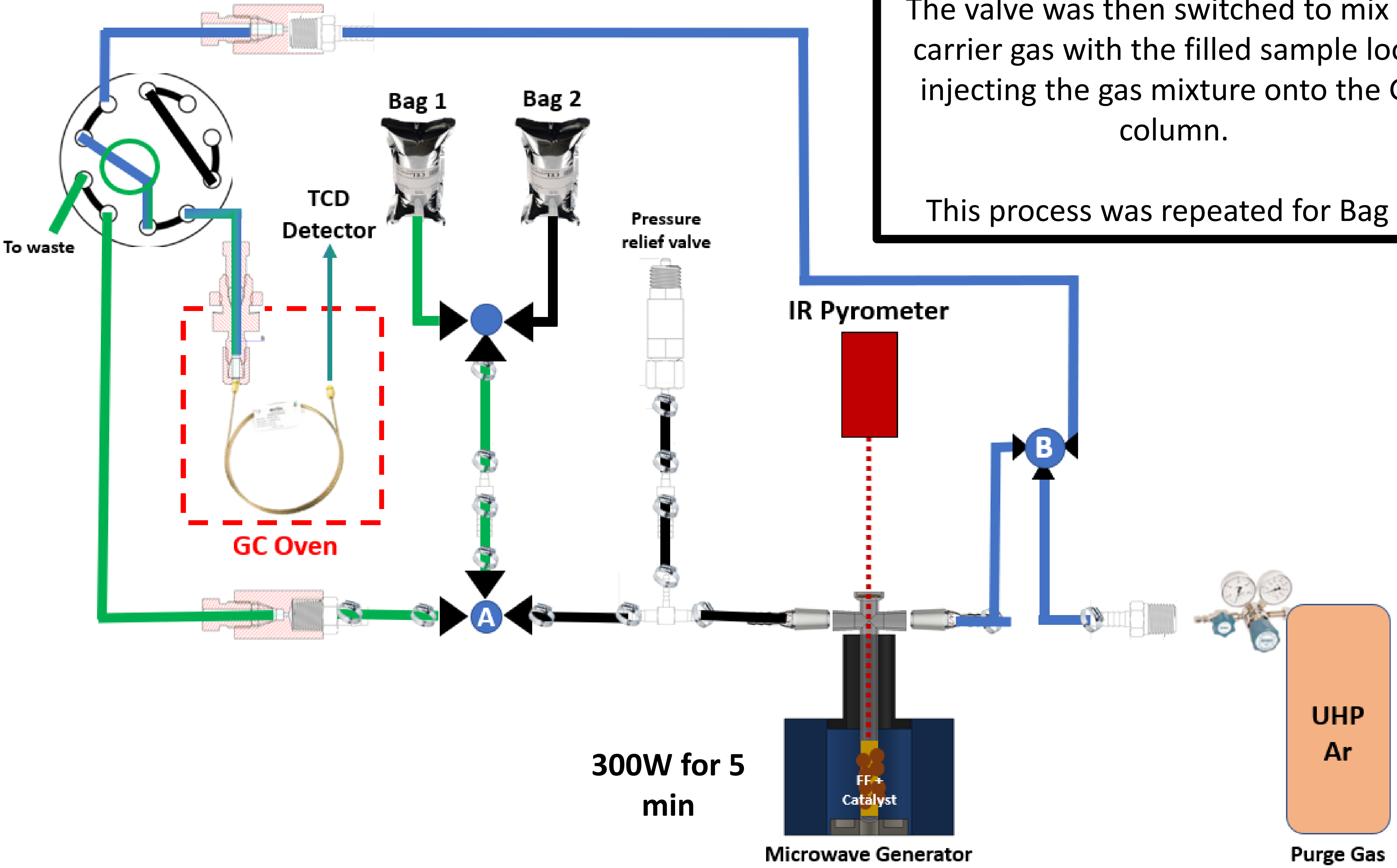

Objective 2

Dehydrogenation procedure

Objective 2

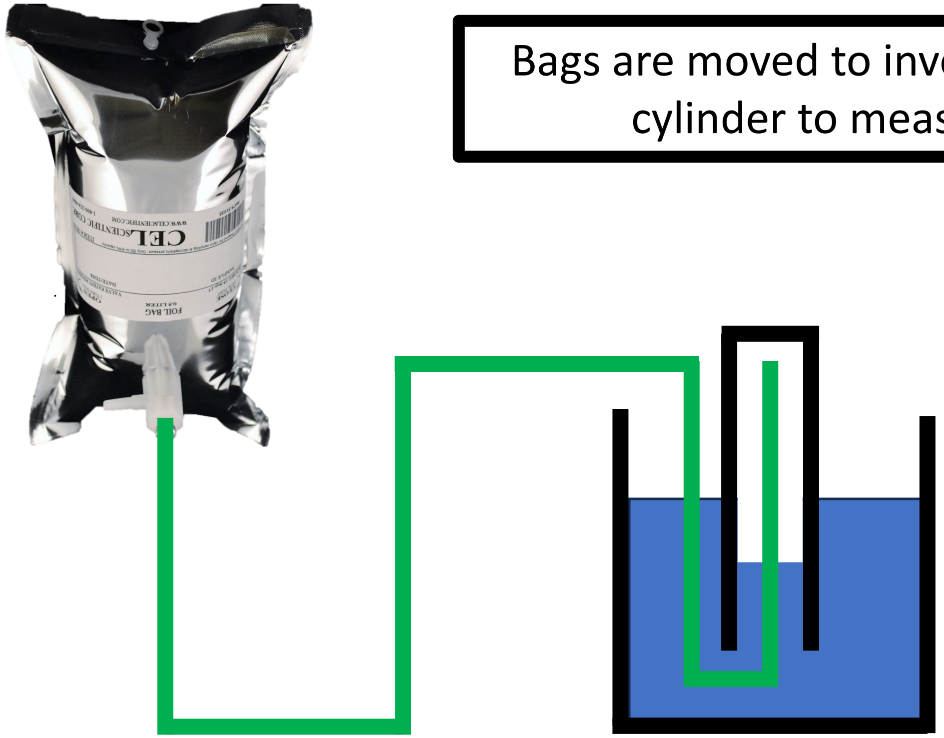

Bags are moved to inverted graduated cylinder to measure yield.

Diesel dehydrogenation – SCS fuel

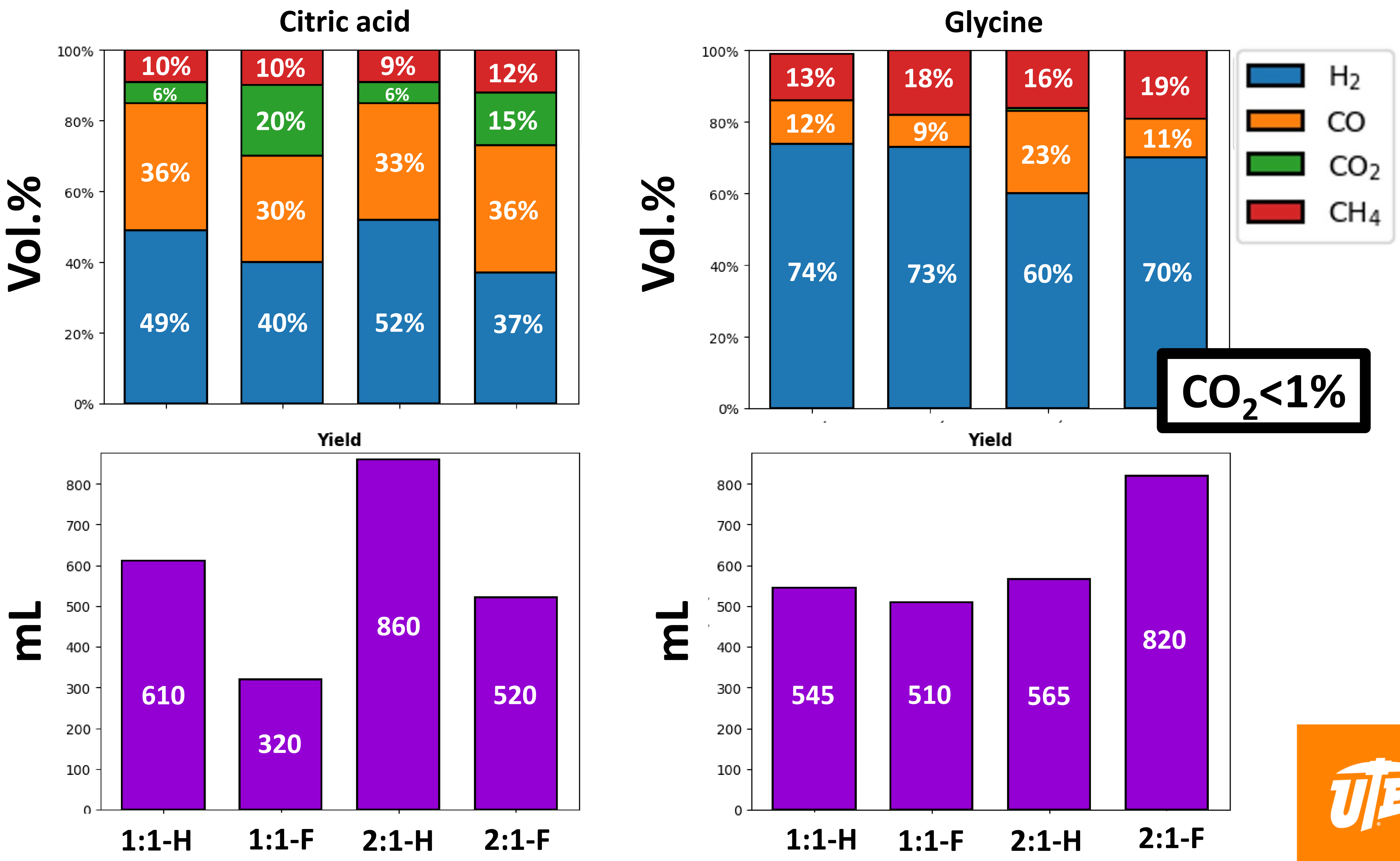

Diesel dehydrogenation – SCS Fe:Al ratio

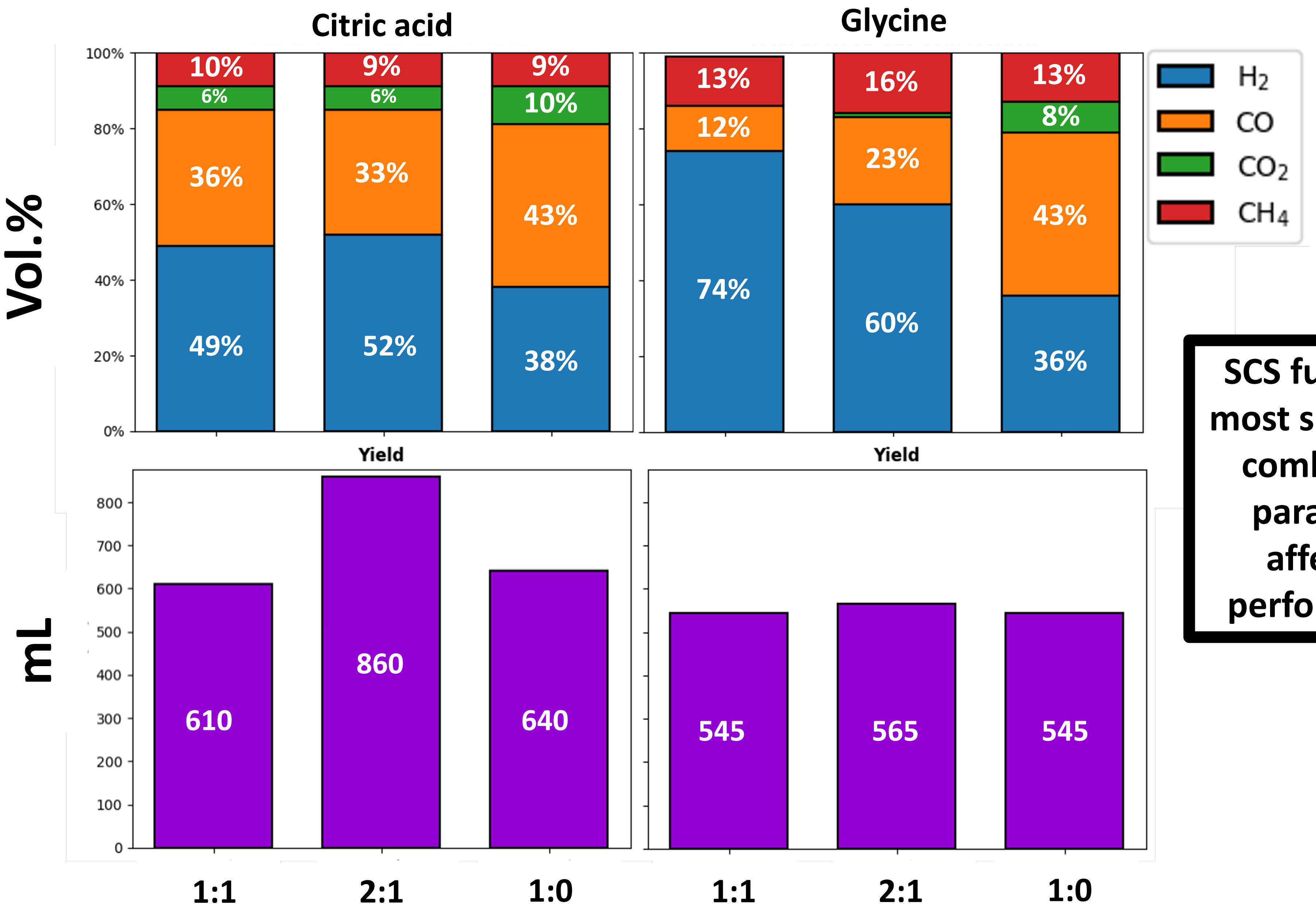

SCS fuel is the most significant combustion parameter affecting performance.

Diesel vs. gasoline dehydrogenation

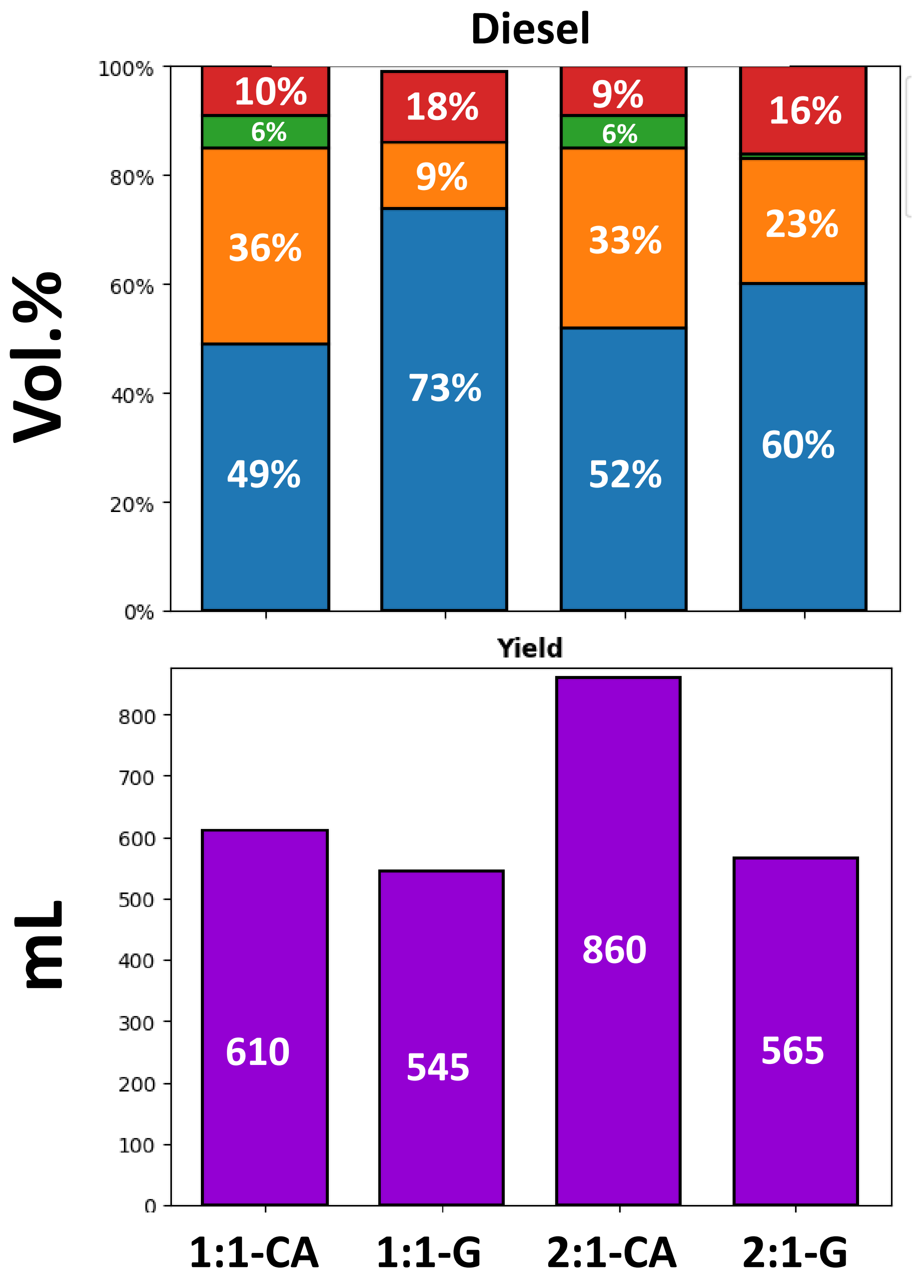

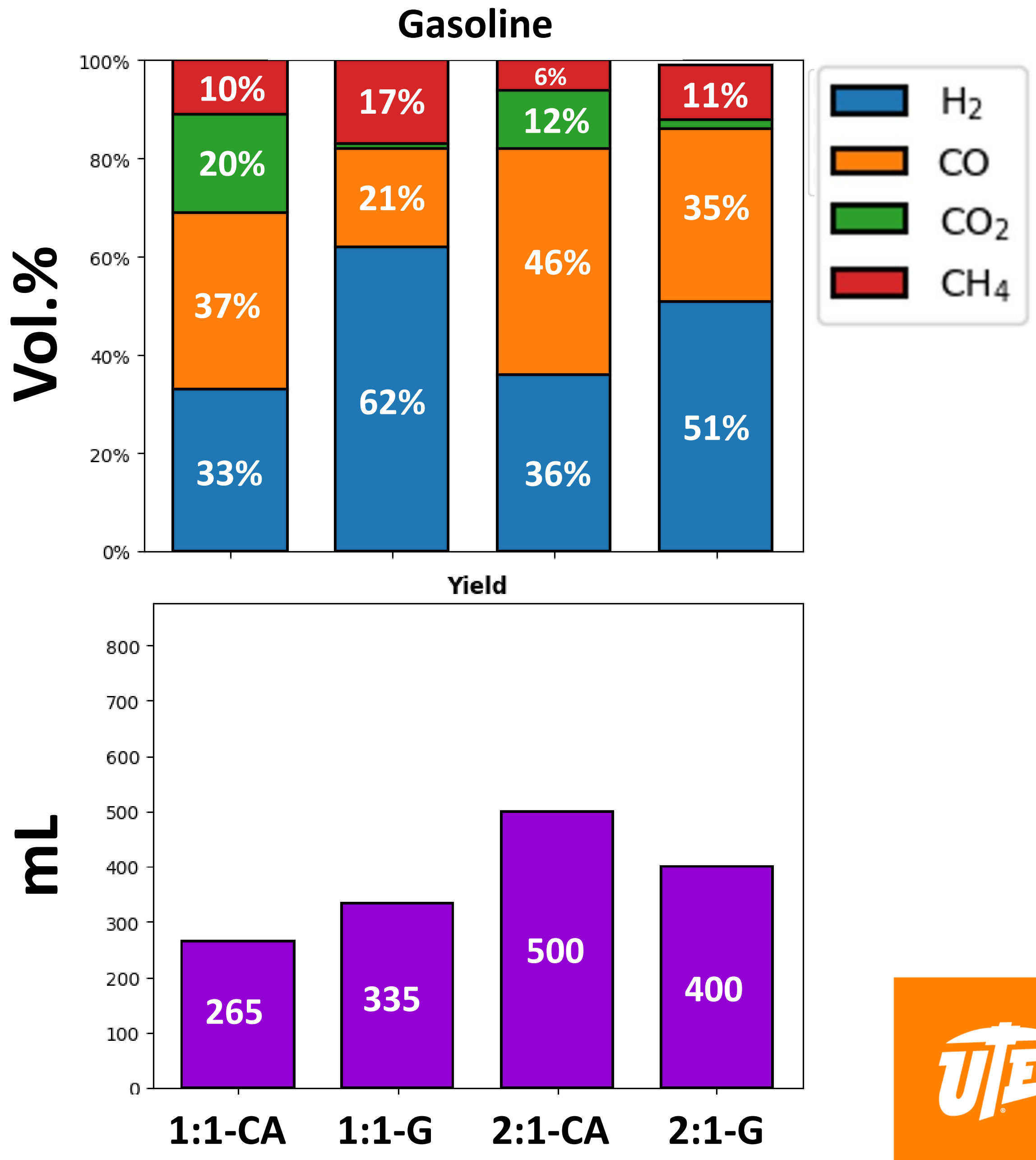

Objective 2

Post dehydrogenation – XRD characterization

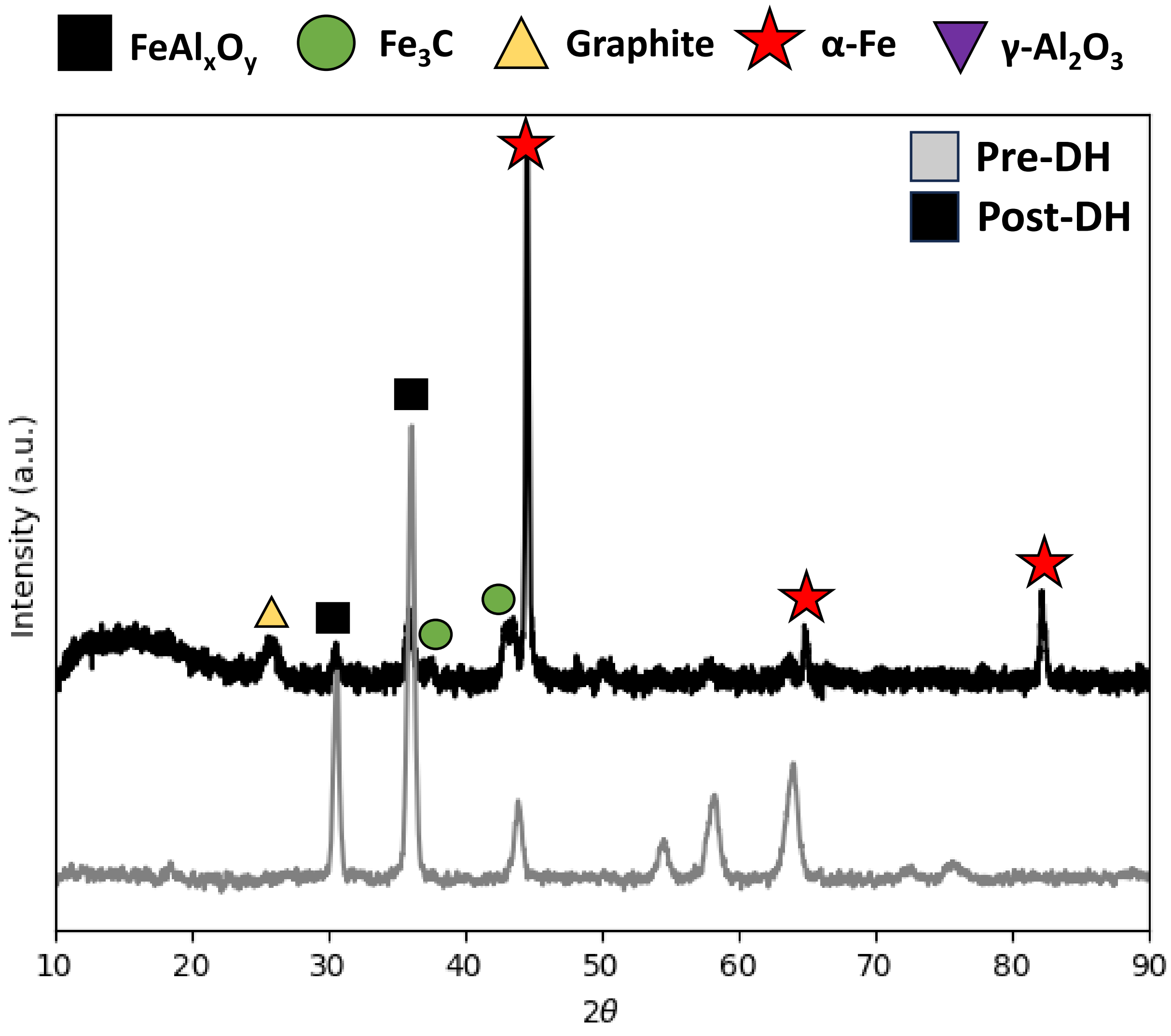

2:1-G

	Pre-DH $FeAl_xO_y$ (311)	Post-DH $FeAl_xO_y$ (311)
Lattice parameter (Å)	8.21	8.27
Crystallite size (nm)	12.5	13.5

Post dehydrogenation – XRD characterization

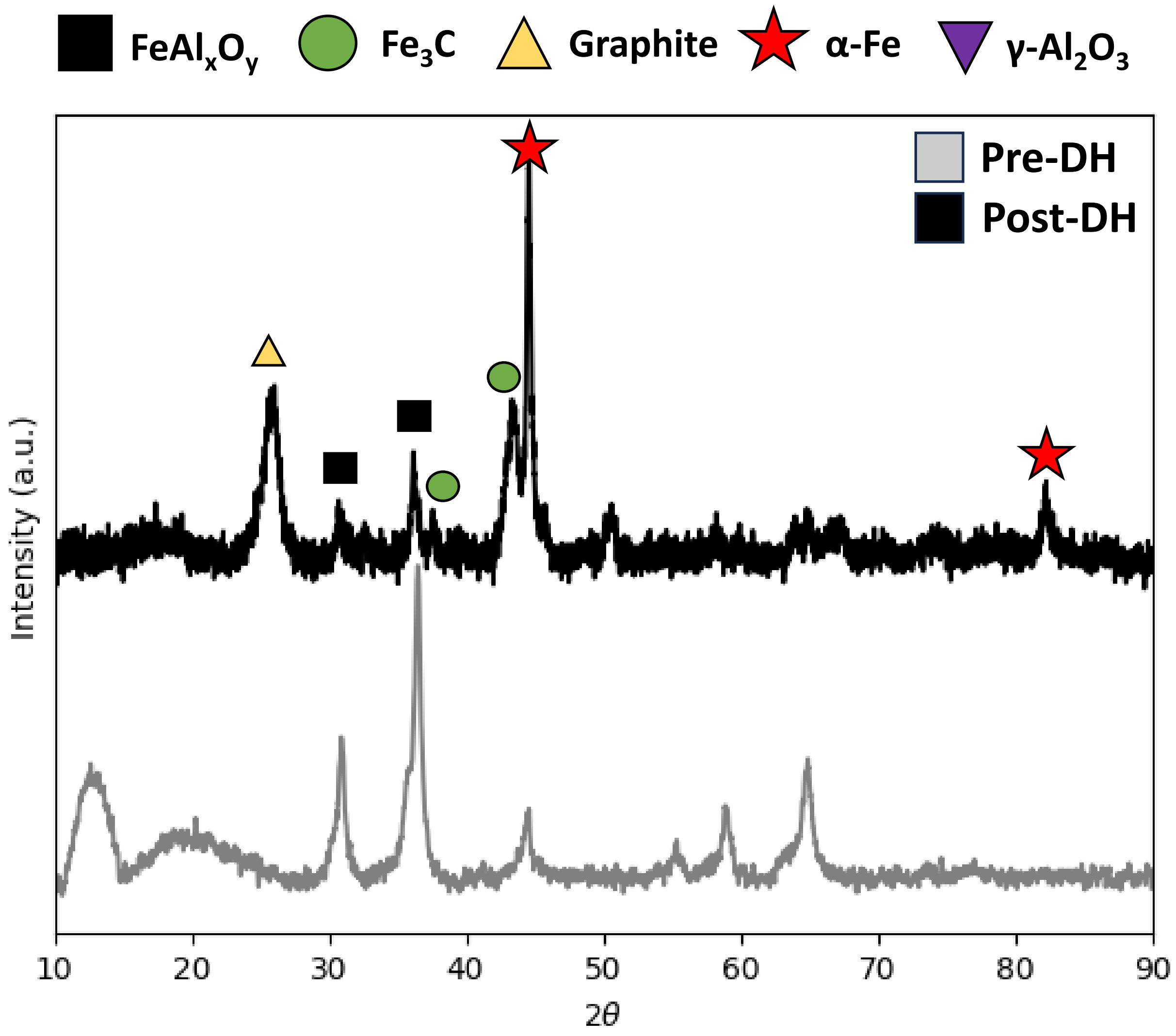

1:1-G

	Pre-DH $FeAl_xO_y$ (311)	Post-DH $FeAl_xO_y$ (311)
Lattice parameter (Å)	8.20	8.22
Crystallite size (nm)	9.5	14.2

Post dehydrogenation – XRD characterization

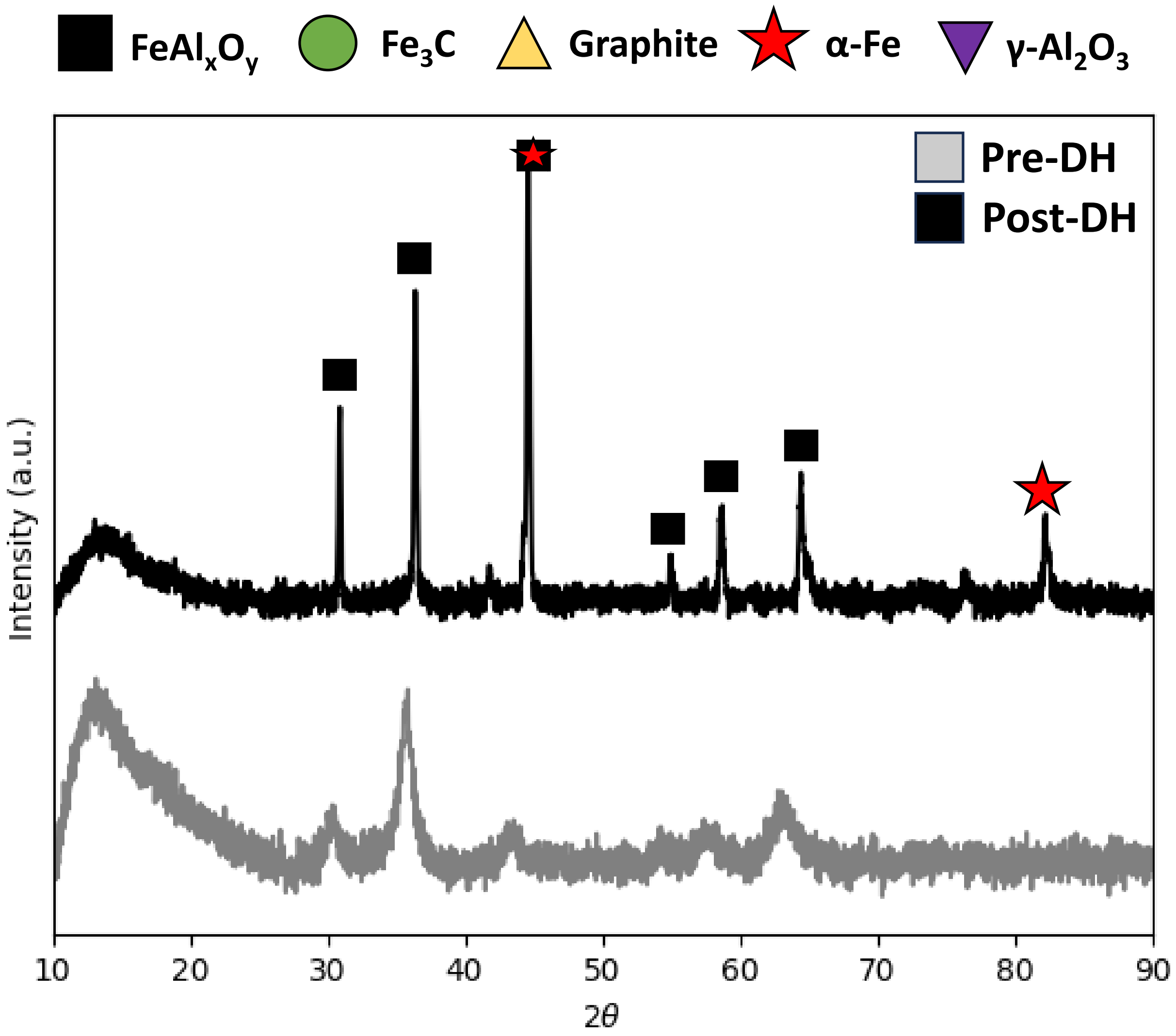

2:1-CA

	Pre-DH FeAl$_x$O$_y$ (311)	Post-DH FeAl$_x$O$_y$ (311)
Lattice parameter (Å)	8.33	8.18
Crystallite size (nm)	6.4	33.6

Objective 2

Objective 2

Post dehydrogenation – XRD characterization

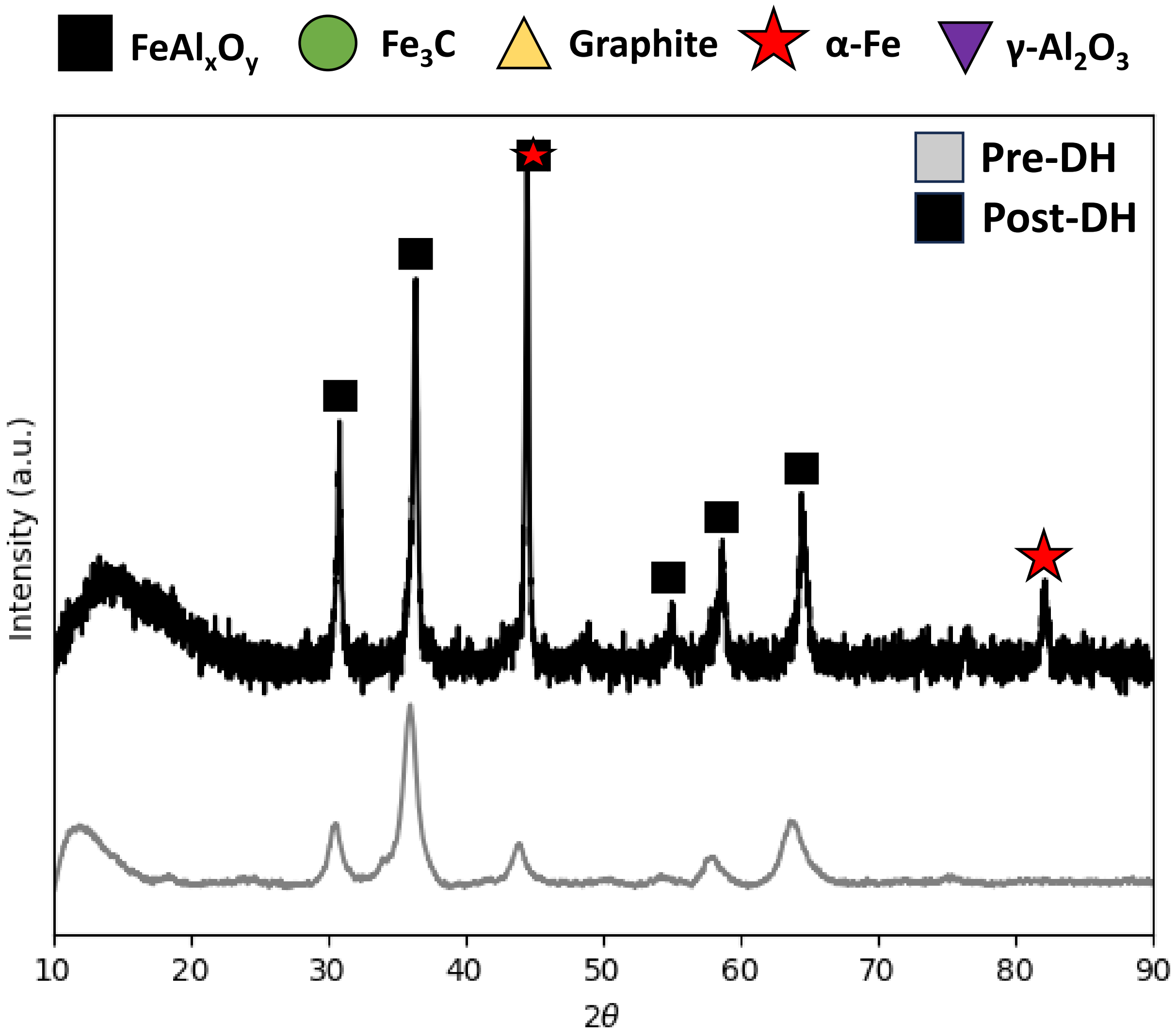

1:1-CA

	Pre-DH $FeAl_xO_y$ (311)	Post-DH $FeAl_xO_y$ (311)
Lattice parameter (Å)	8.27	8.18
Crystallite size (nm)	5.3	16.7

Post dehydrogenation – XRD characterization

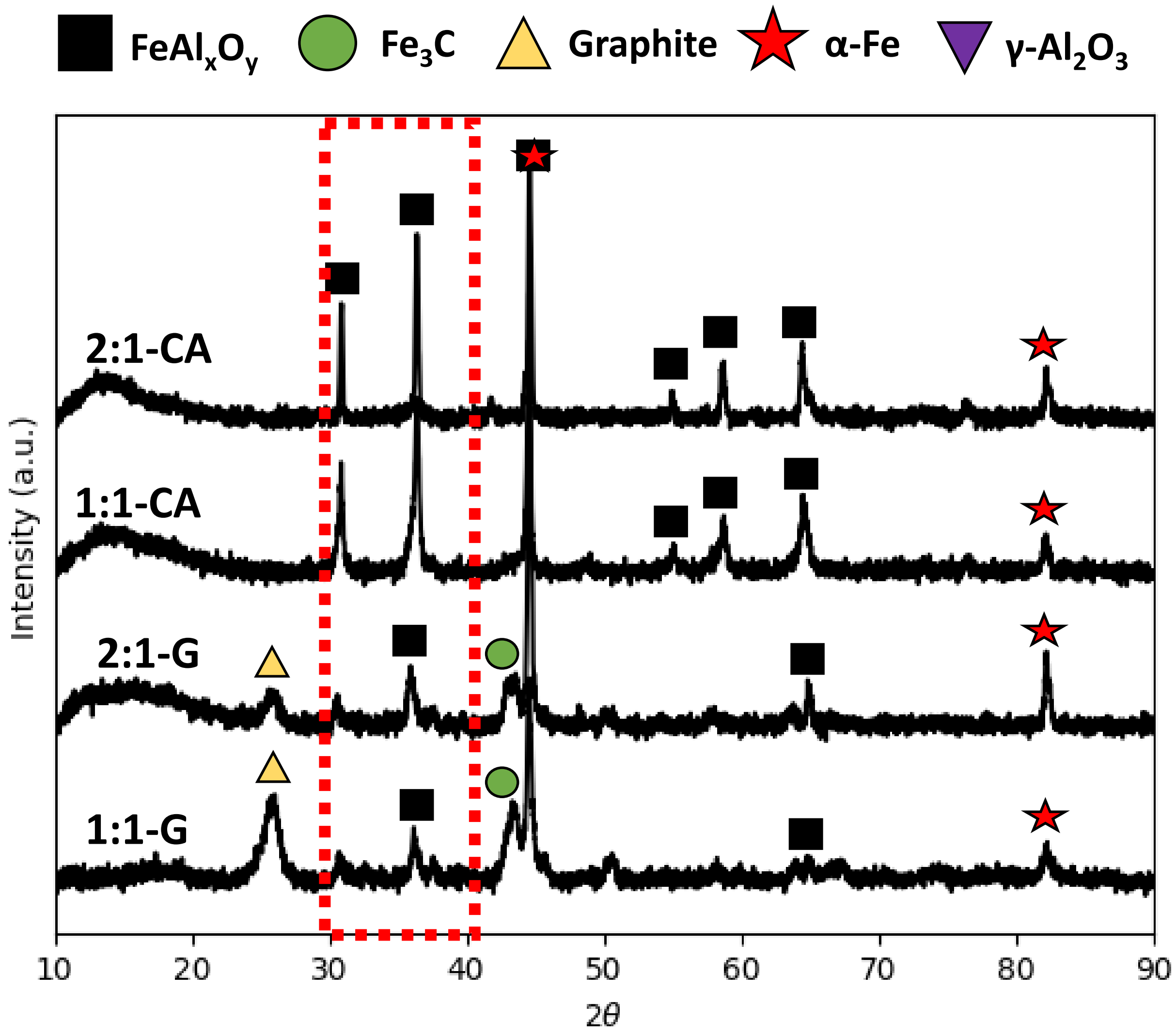

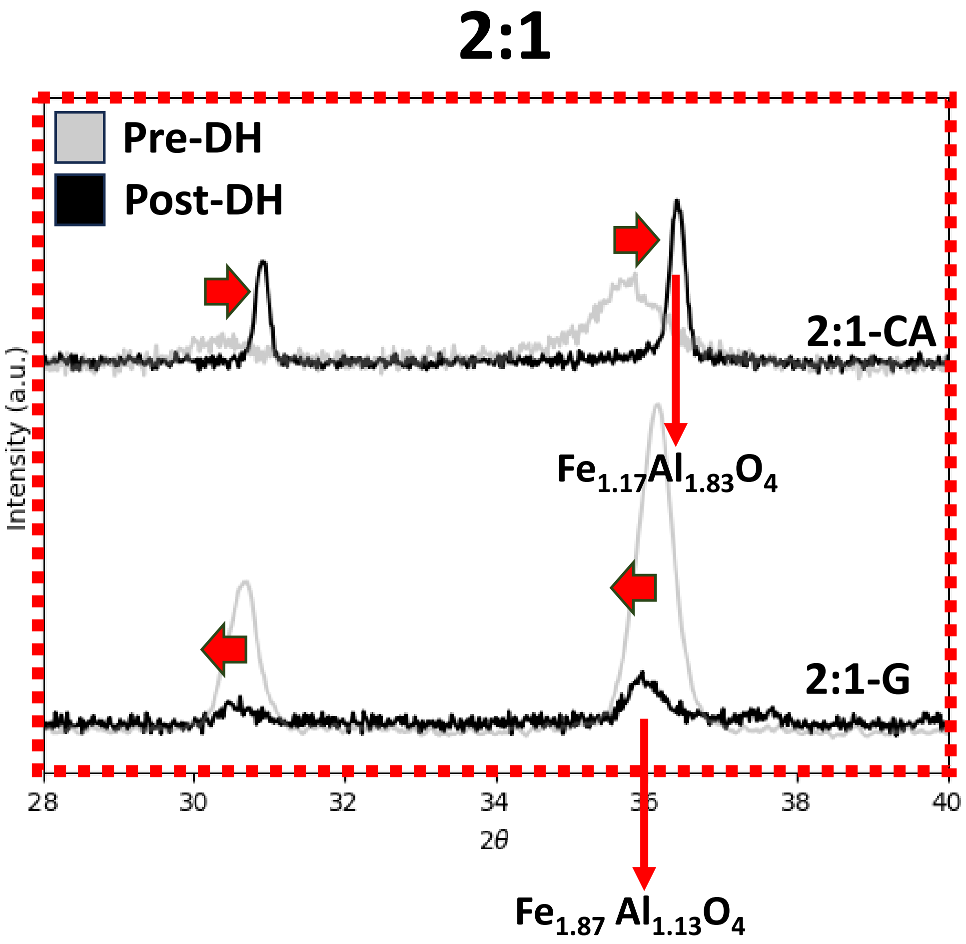

Objective 2

Post dehydrogenation – XRD characterization

Objective 2

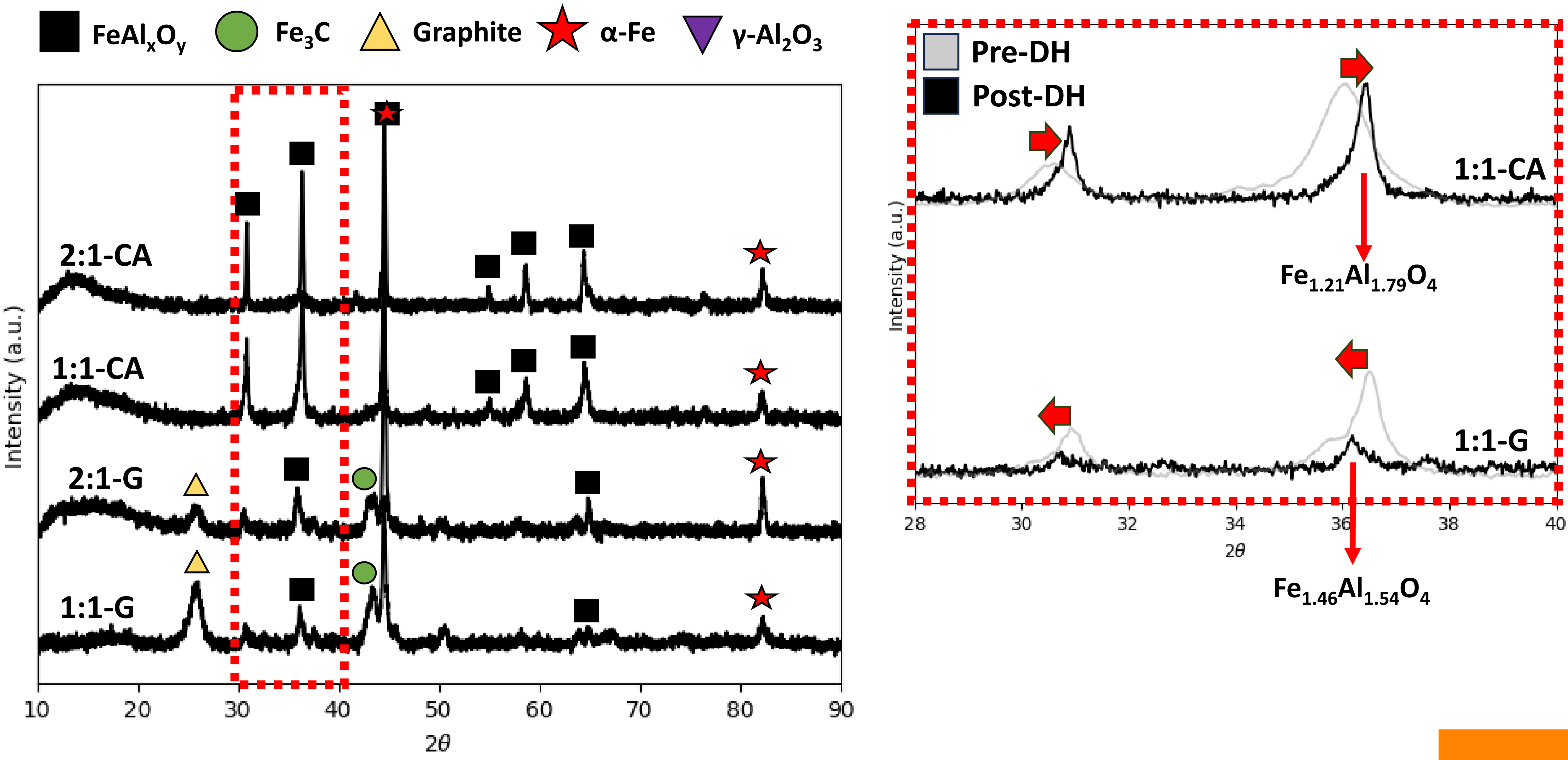

Scanning electron microscopy

2:1-CA-H

Fe	Al	O	C
15 at.%	44 at.%	4 at.%	37 at.%

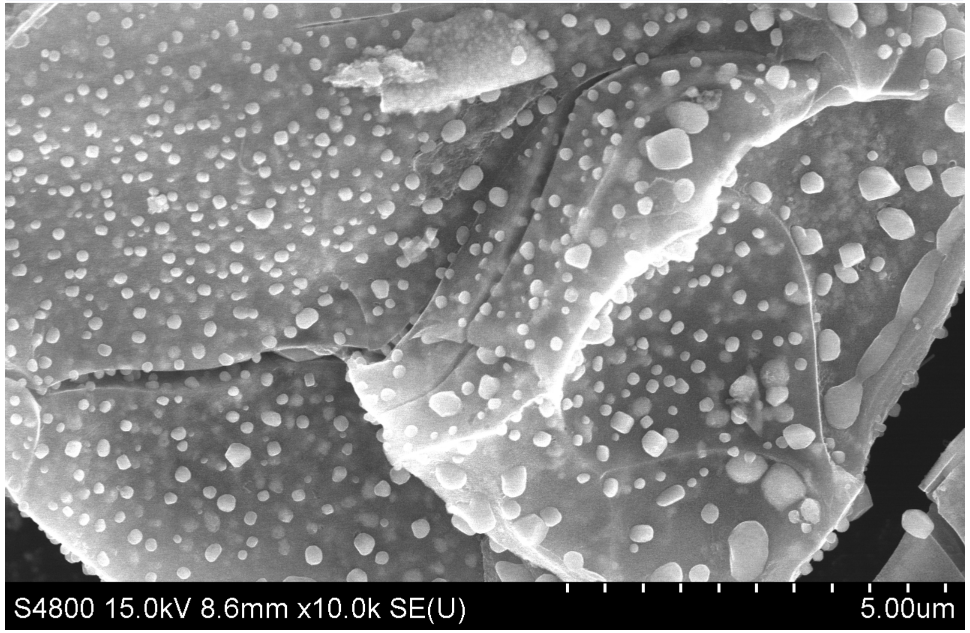

Speckled growth regions

Fe	Al	O	C
11 at.%	34 at.%	17 at.%	38 at.%

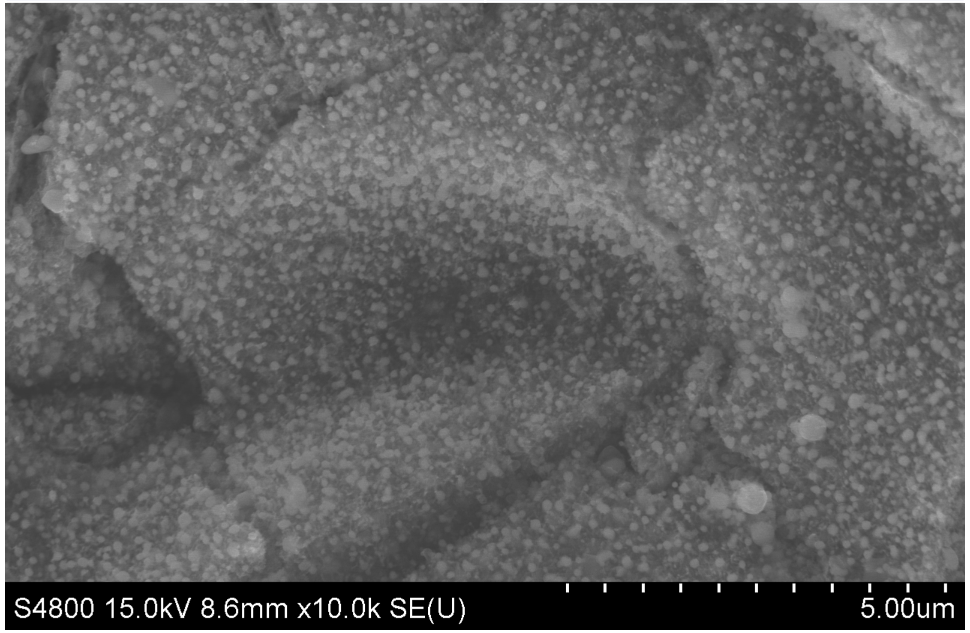

Bulbed regions

Scanning electron microscopy

2:1-CA-H

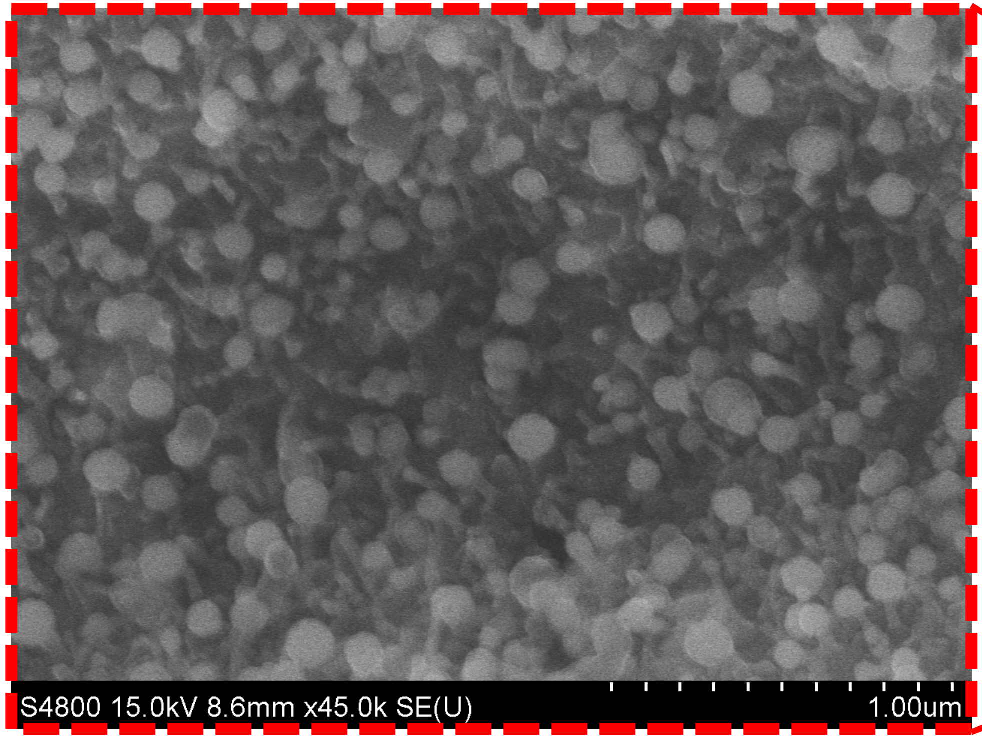

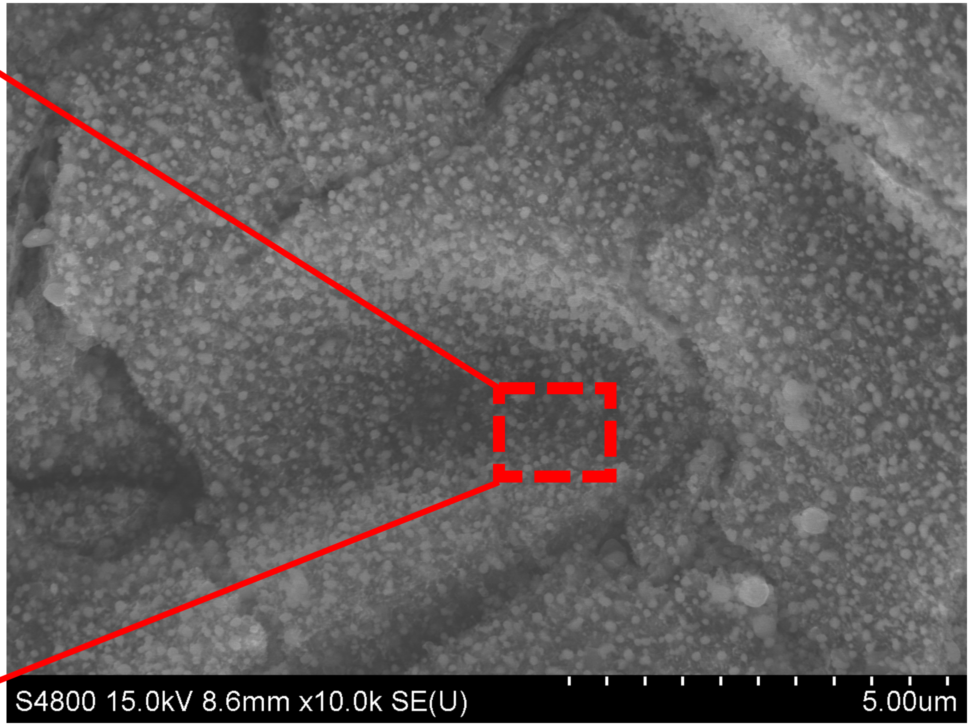

Bulbed regions

Objective 2

Scanning electron microscopy

2:1-CA-H

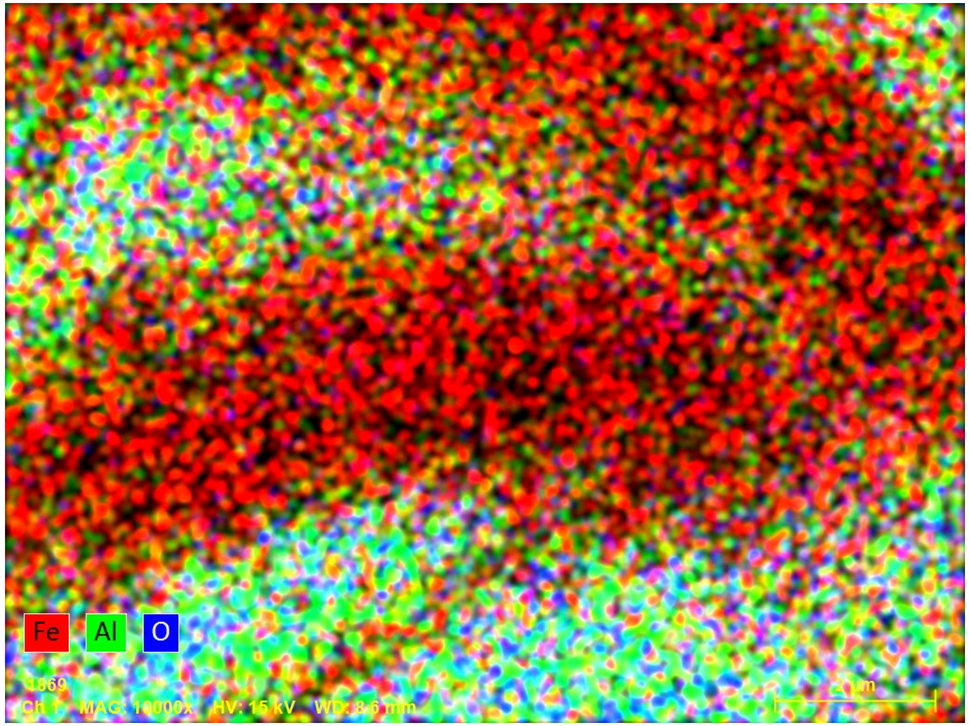

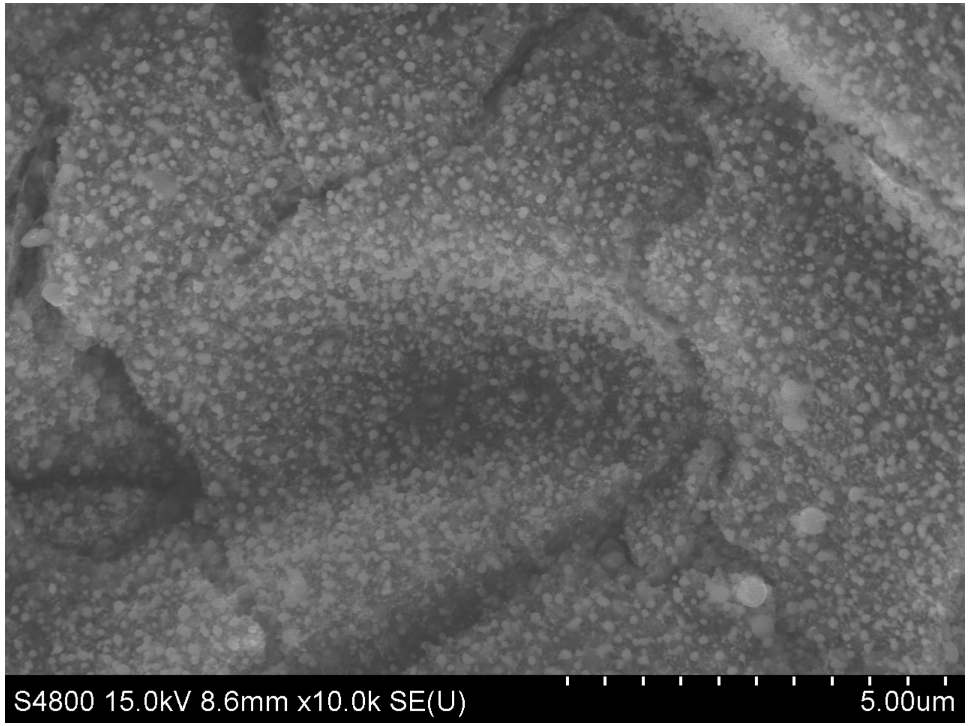

- Segregation of Fe from $FeAl_xO_y$
- Formation of carbon on $FeAl_xO_y$ regions

Objective 2

Scanning electron microscopy

2:1-CA-H

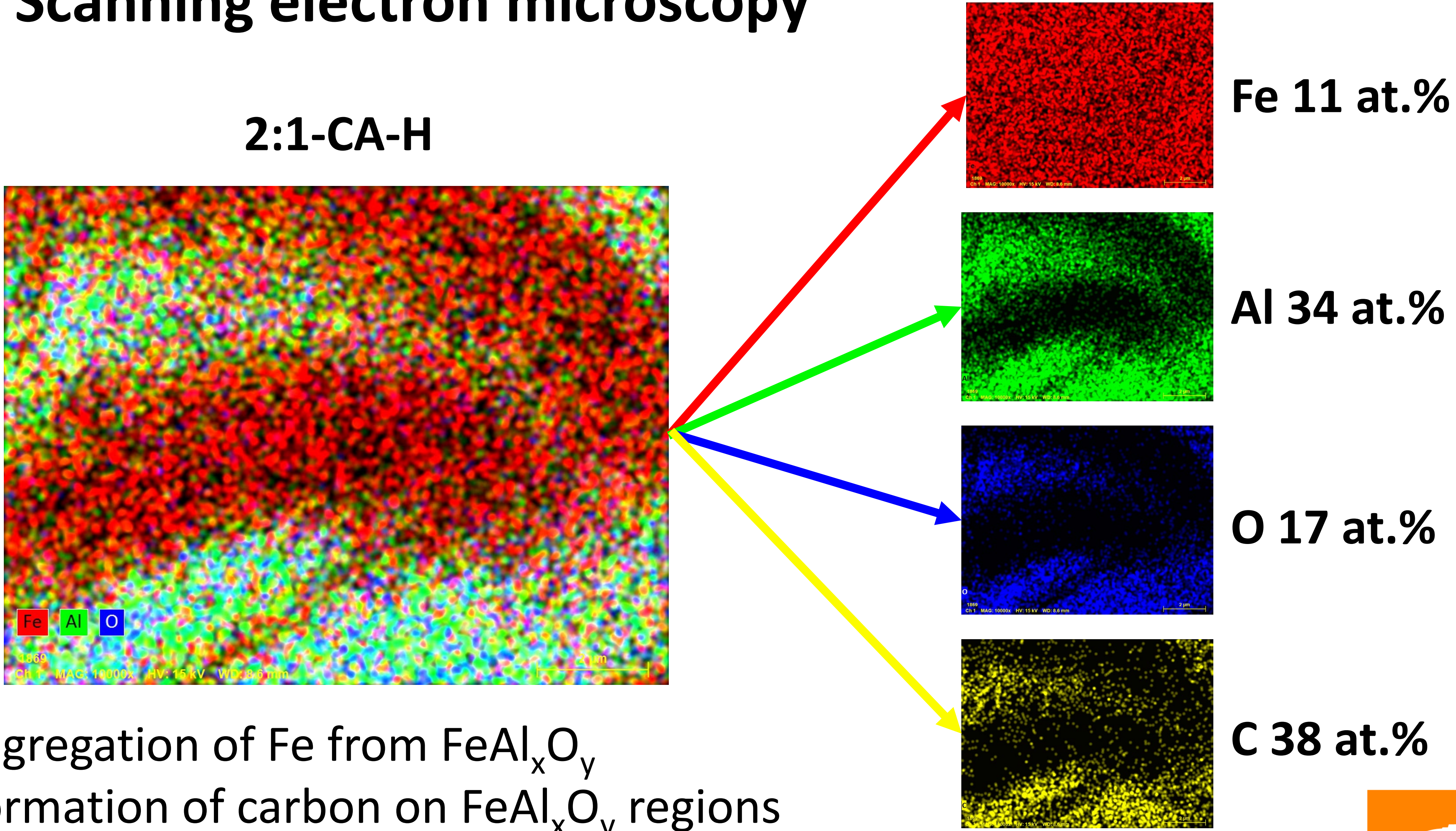

- Segregation of Fe from $FeAl_xO_y$
- Formation of carbon on $FeAl_xO_y$ regions

Objective 2

Scanning electron microscopy

2:1-CA-H

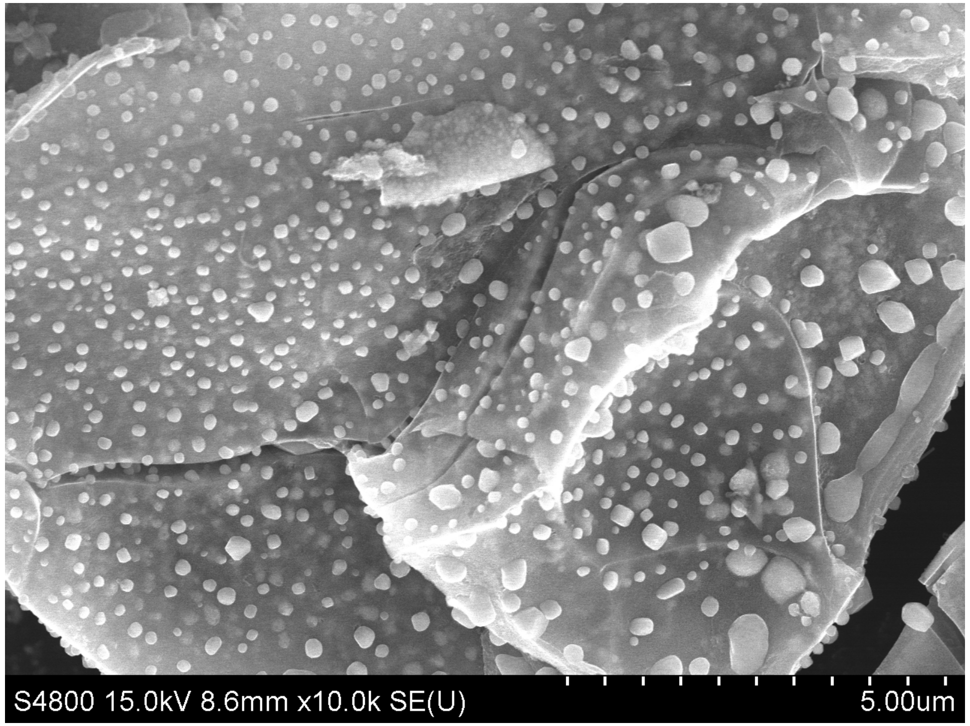

2:1-G-H

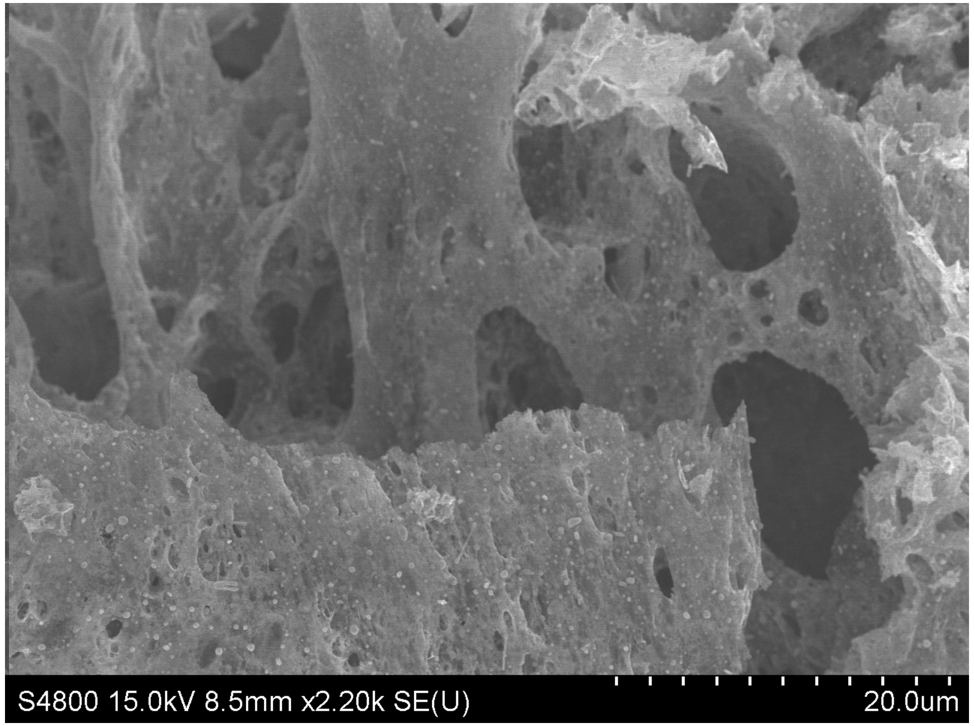

- Some regions of G-derived products retained their porous structure seen before dehydrogenation.

Scanning electron microscopy

Objective 2

2:1-CA-H

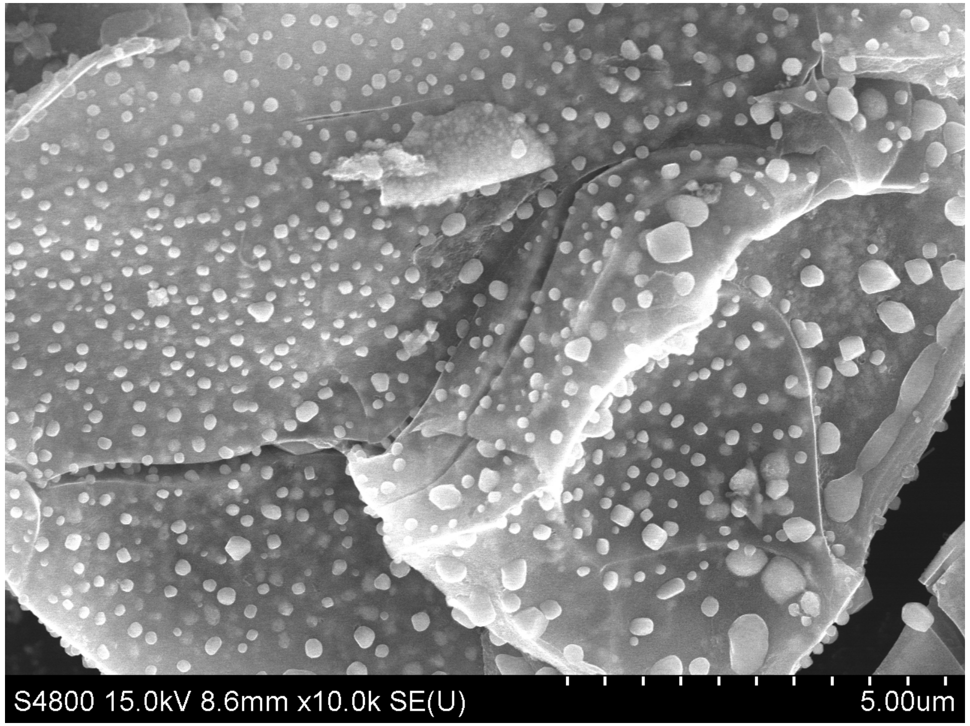

2:1-G-H

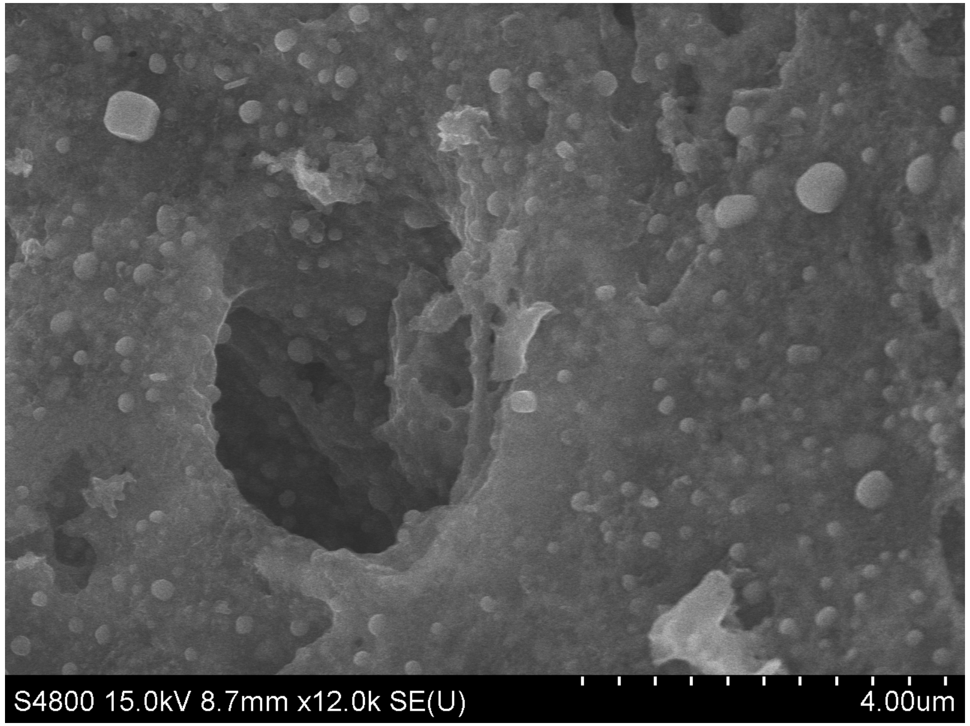

- However, other regions looked like CA-derived products but with less speckles.

Objective 2

Scanning electron microscopy

2:1-CA-H

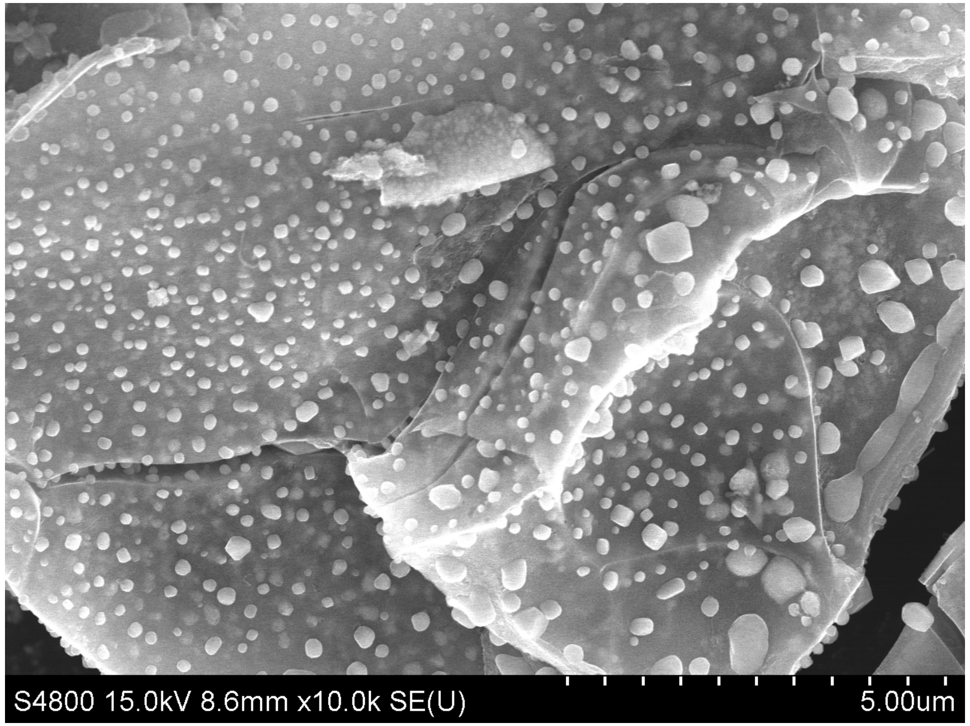

2:1-G-H

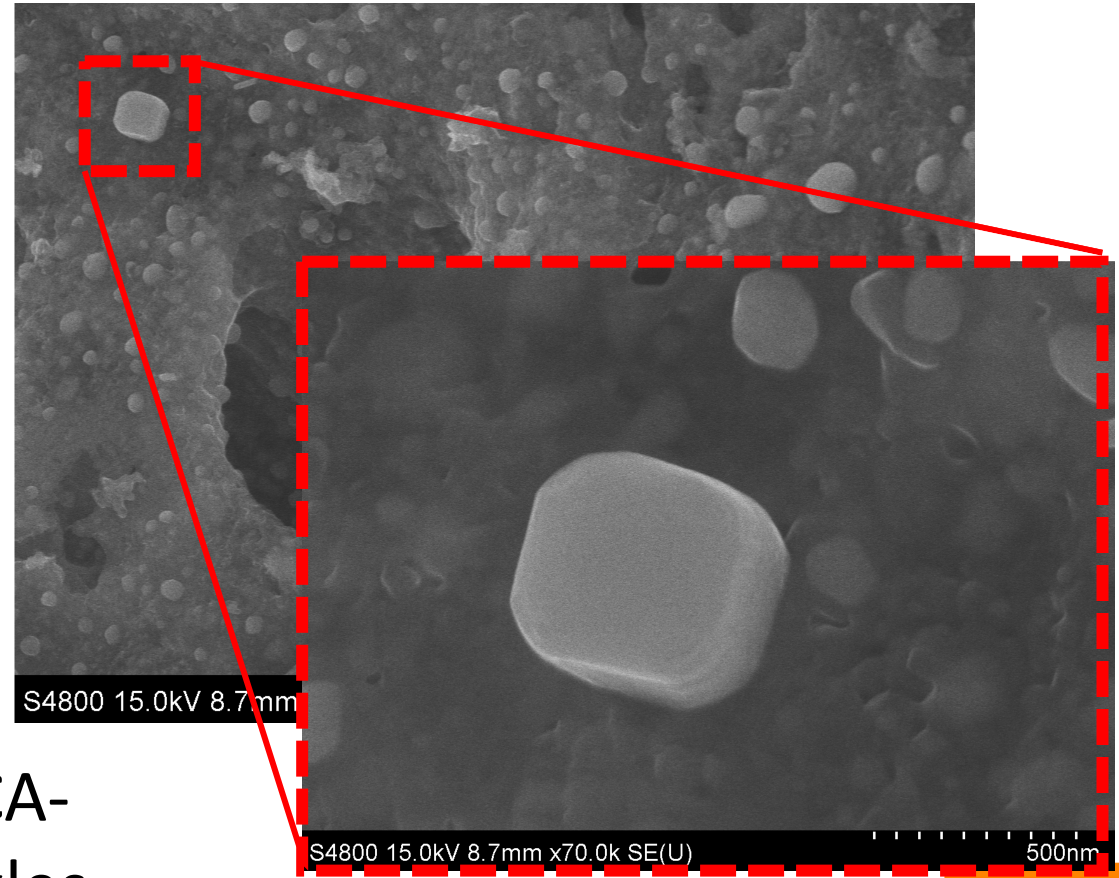

- However, other regions looked like CA-derived products but with less speckles.

Scanning electron microscopy

2:1-G-H

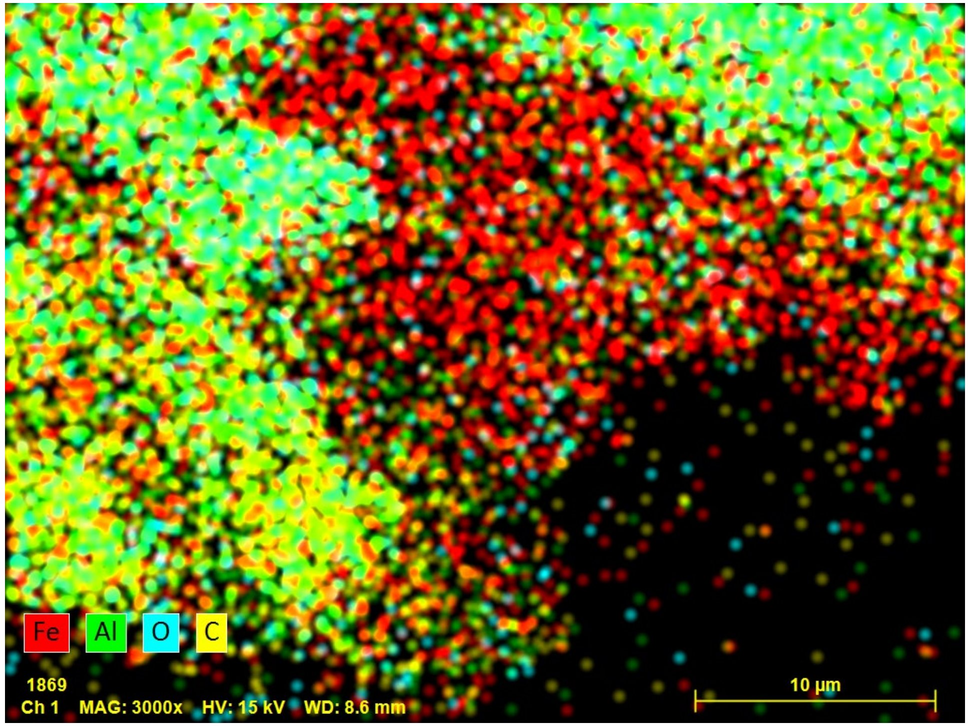

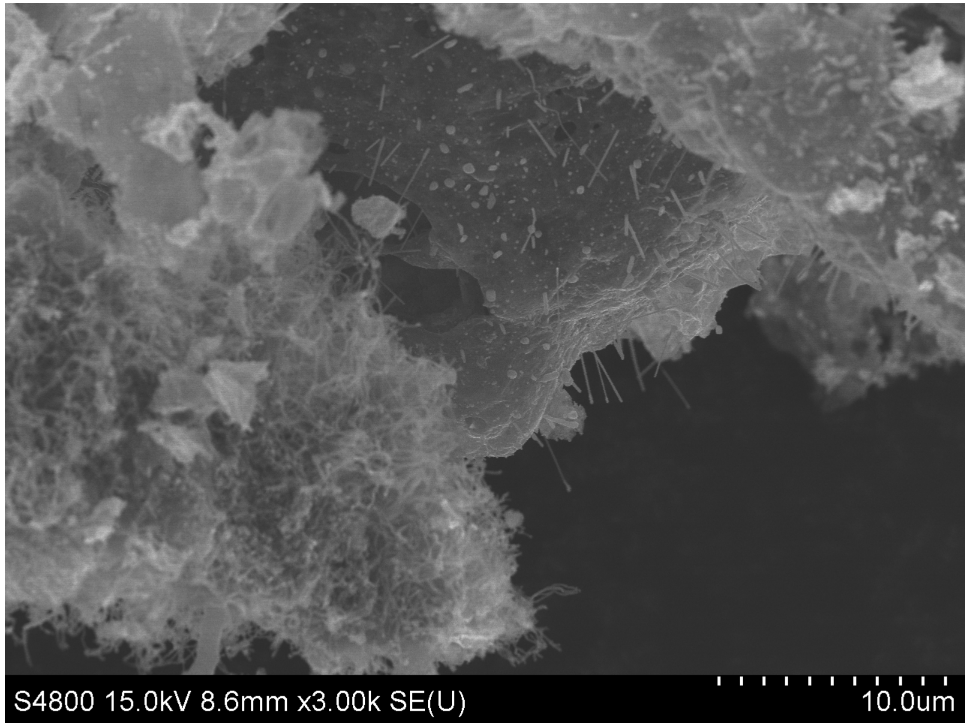

- Visible regions of substantial carbon nanotube growth

Objective 2

Scanning electron microscopy

2:1-G-H

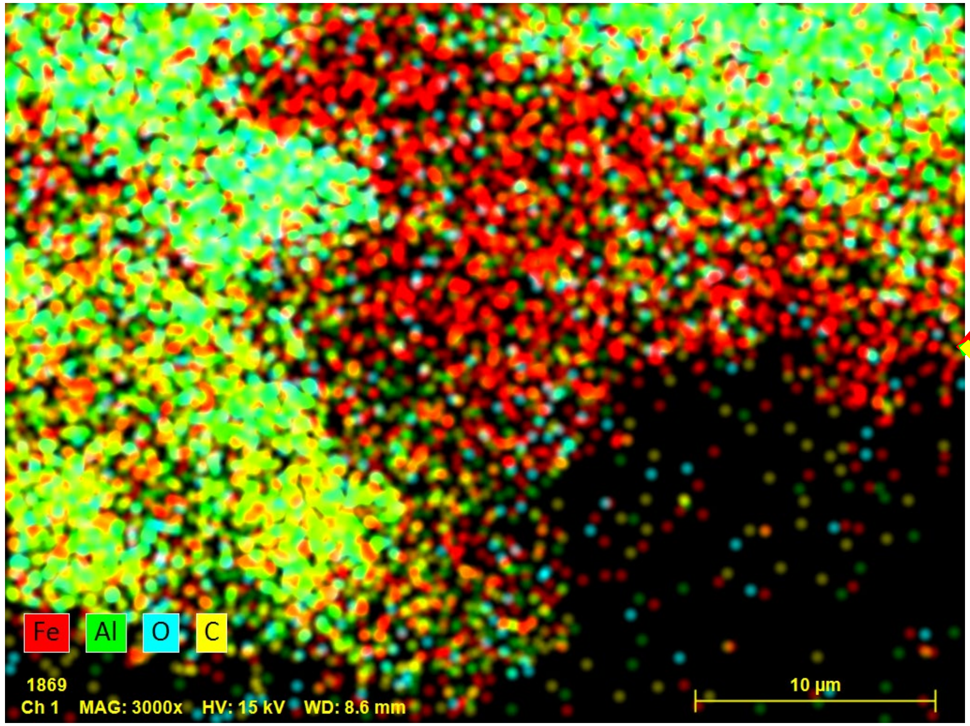

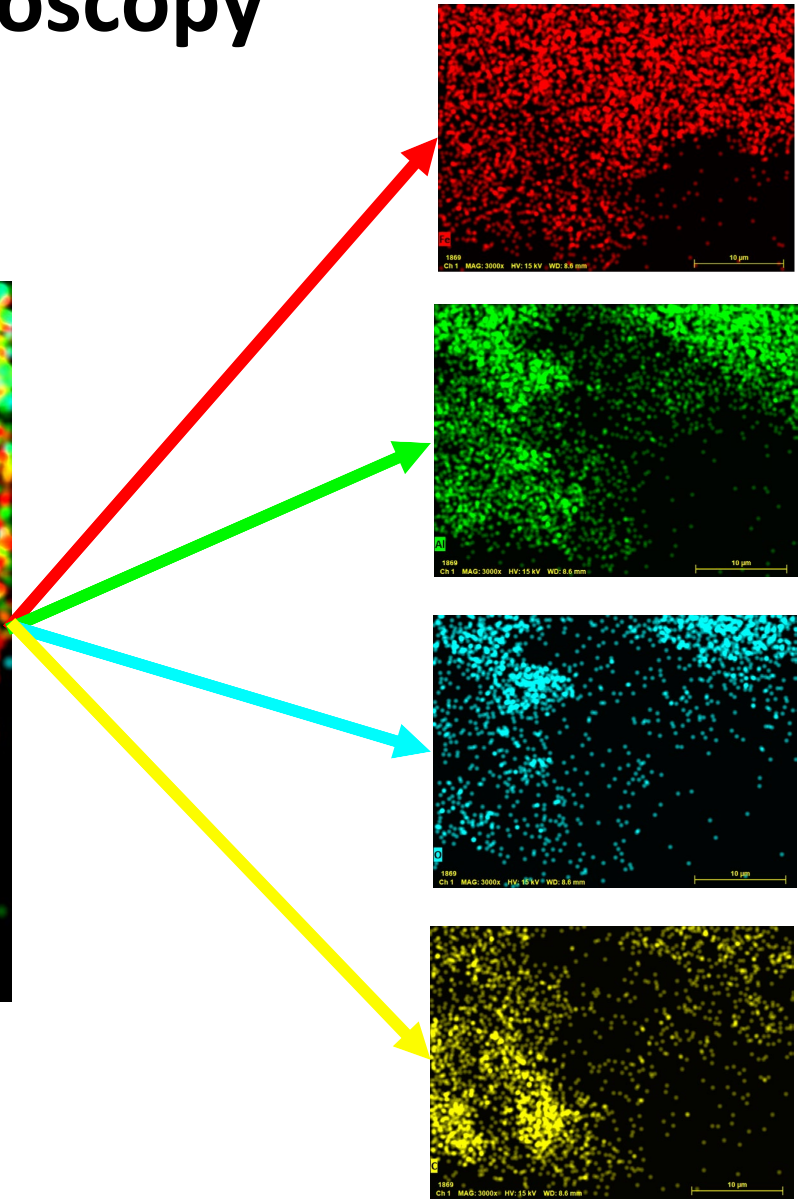

Fe 7 at.%

Al 22 at.%

O 15 at.%

C 56 at.%

- Visible regions of substantial carbon nanotube growth

Scanning electron microscopy

Objective 2

2:1-G-H

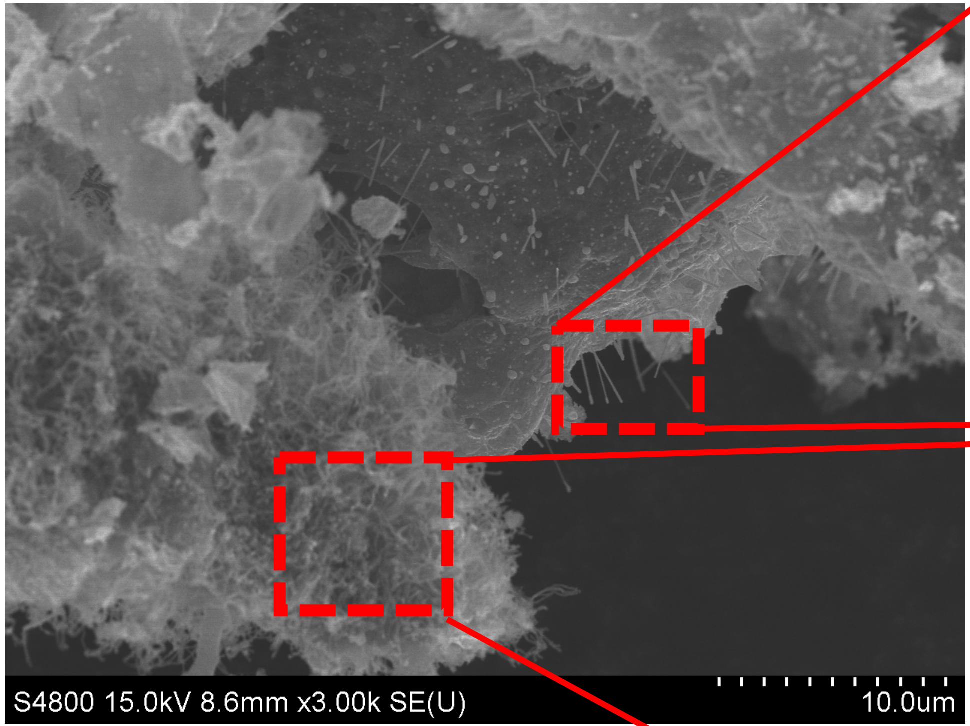

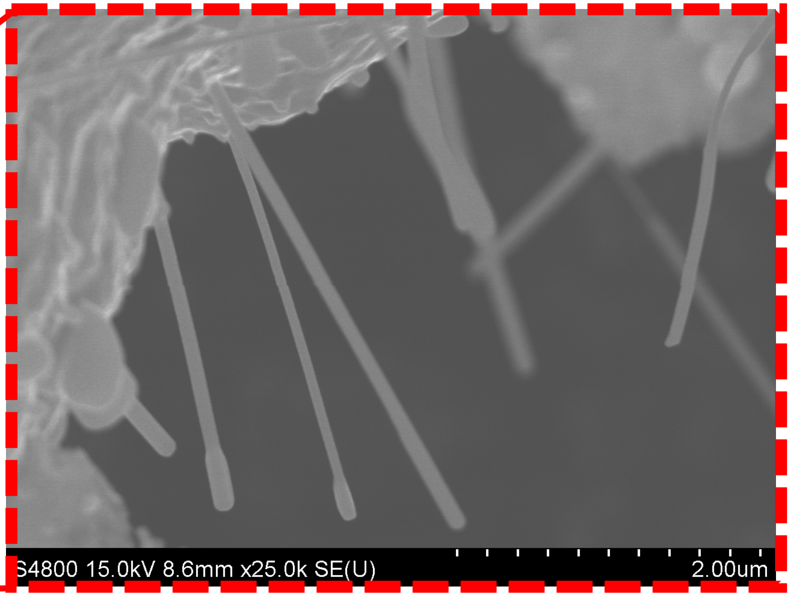

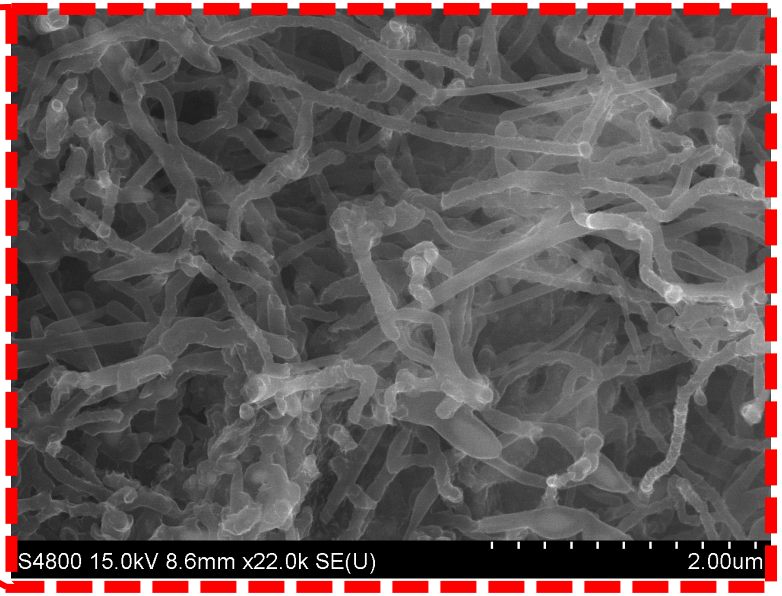

- Visible regions of substantial carbon nanotube growth

Scanning electron microscopy

1:1-CA-H

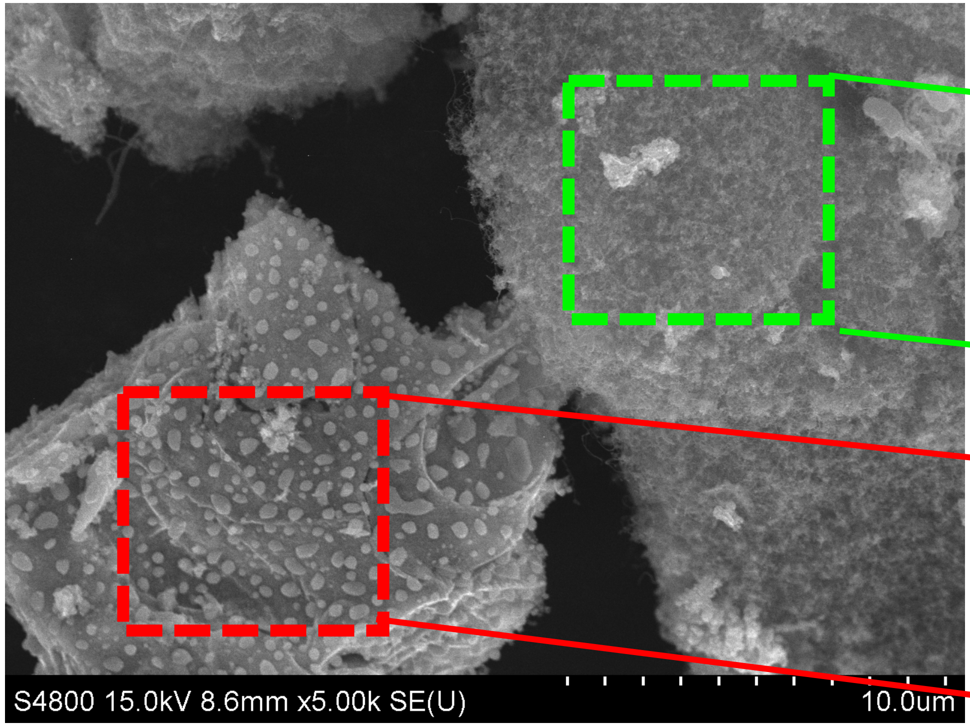

Fe	Al	O	C
10 at.%	17 at.%	4 at.%	58 at.%

Fe	Al	O	C
40 at.%	30 at.%	5 at.%	25 at.%

- CA-derived products appeared to have less regions of carbon nanotubes.

Catalyst regeneration

- Deactivation of catalysts in microwave-assisted reactions is due to two main reasons:
  - Accumulation of solid carbon (coking)
  - Formation of microwave-reflecting phases **like α-Fe.**

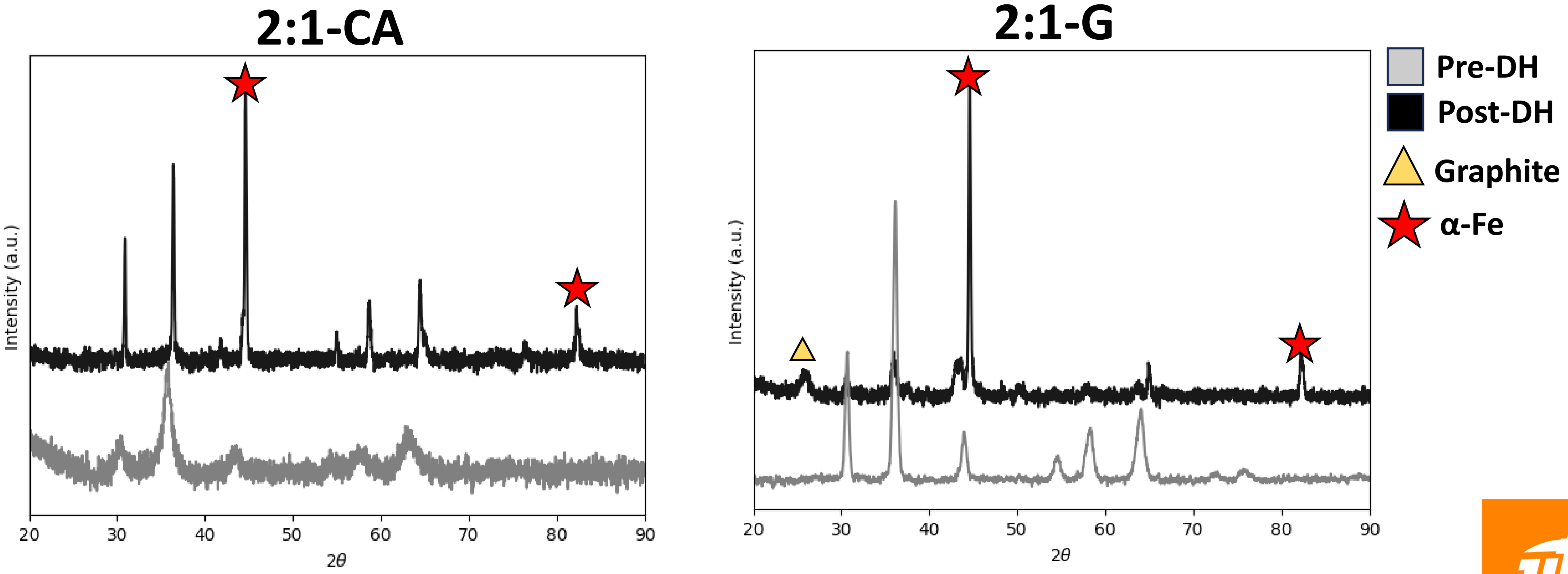

Magnetic separation for catalyst regeneration

- As seen with SEM, the growth of carbon nanotubes on the extremely **magnetic** metallic iron made magnetic separation unfeasible.

Objective 3

Post-dehydrogenation catalyst

Entire body is magnetic

Boudouard reaction for catalyst regeneration

- At **high temperatures**, Boudouard reaction consumes solid carbon and CO_2 forming CO:

$$\mathrm{C} + \mathrm{CO_2} \rightleftharpoons \mathrm{CO}$$

- In a tube furnace, we heated spent catalysts for 2 hr at 900°C while flowing CO_2.

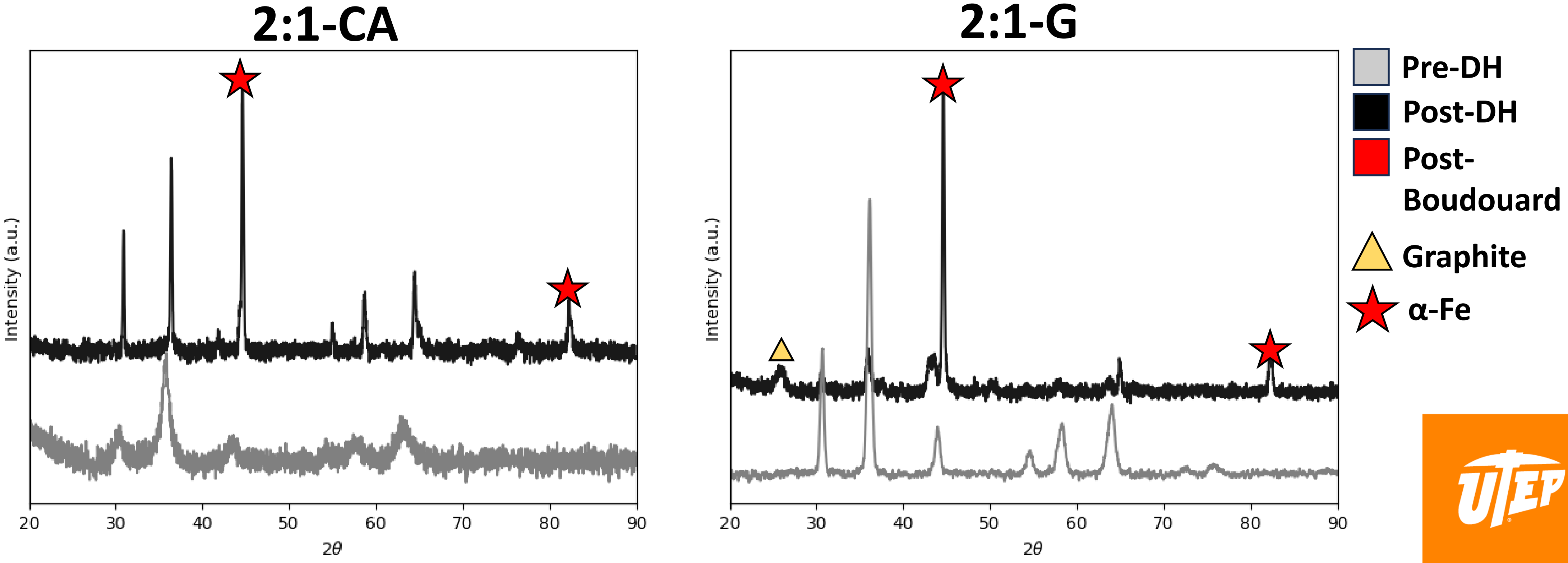

Objective 3

Boudouard reaction for catalyst regeneration

- At **high temperatures**, Boudouard reaction consumes solid carbon and CO_2 forming CO:

$$C + CO_2 \rightleftharpoons CO$$

- In a tube furnace, we heated spent catalysts for 2 hr at 900°C while flowing CO_2.

Removal of carbon and dissolving of α-Fe back into $FeAl_xO_y$

2:1-CA **2:1-G**

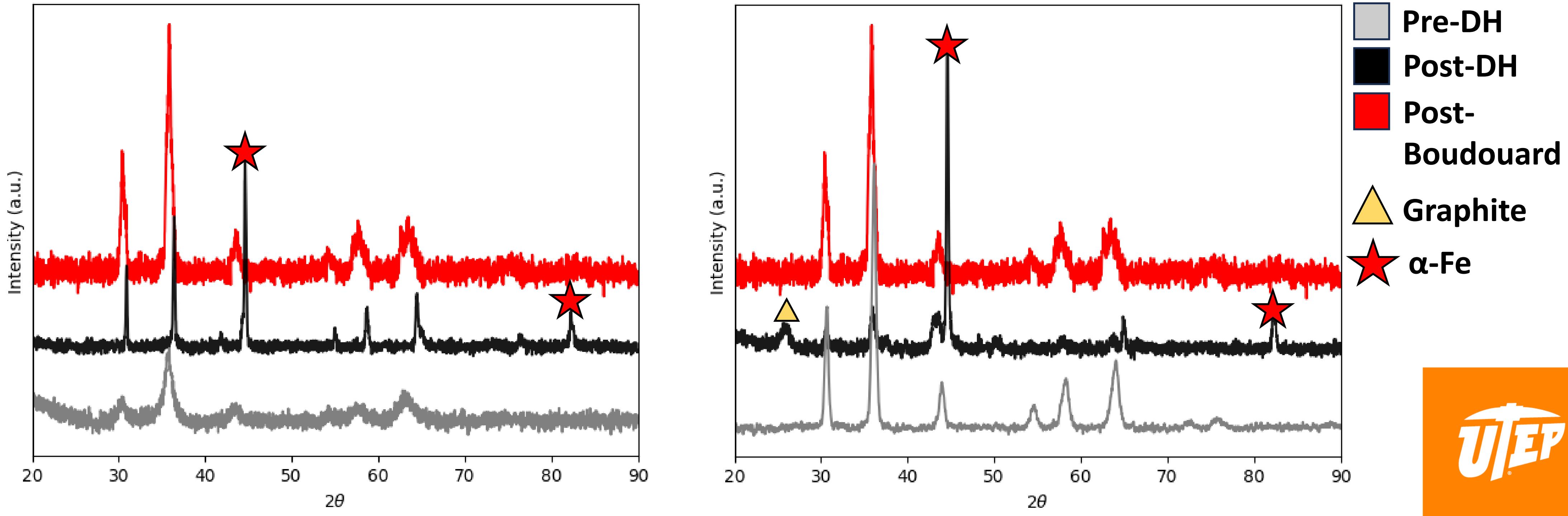

Boudouard reaction for catalyst regeneration

- After Boudouard, the catalysts were reused in a dehydrogenation test.
- Selectivity remained consistent, but yield was lower.
- G-derived catalysts appear more regenerable than CA-derived ones.

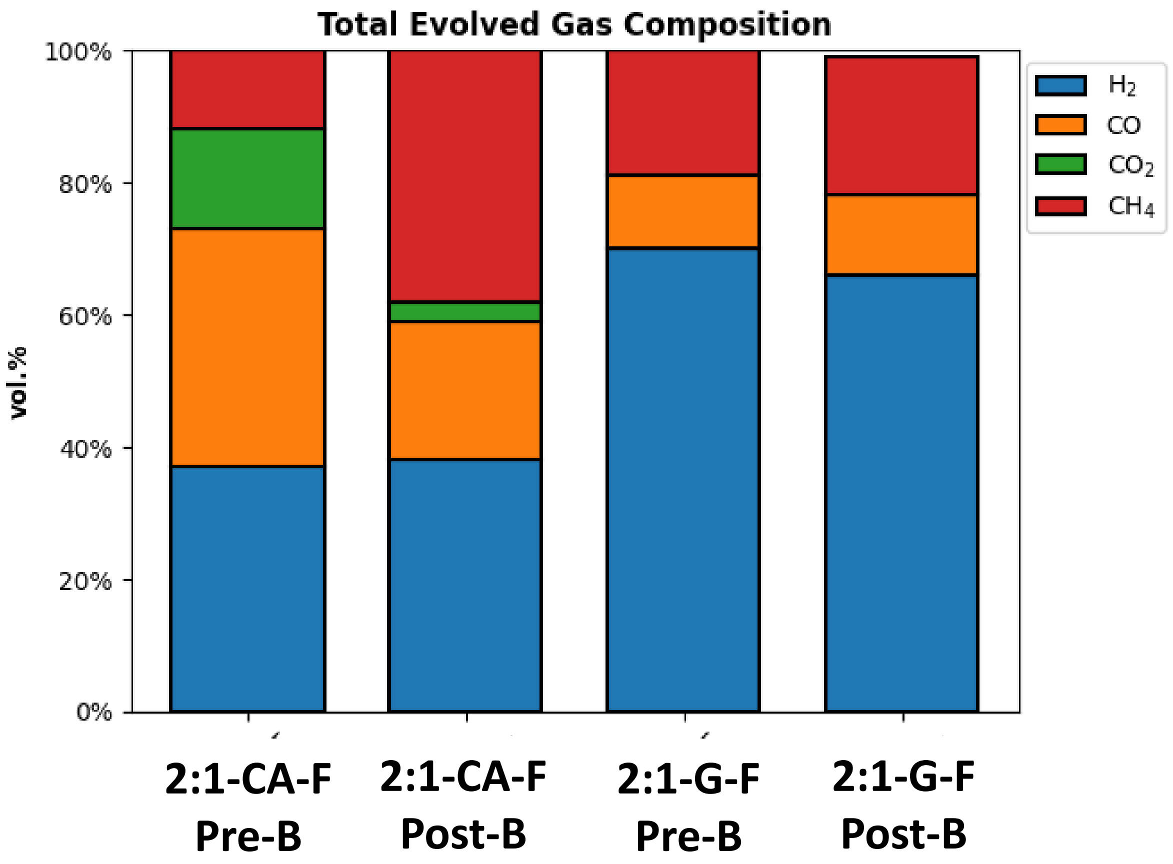

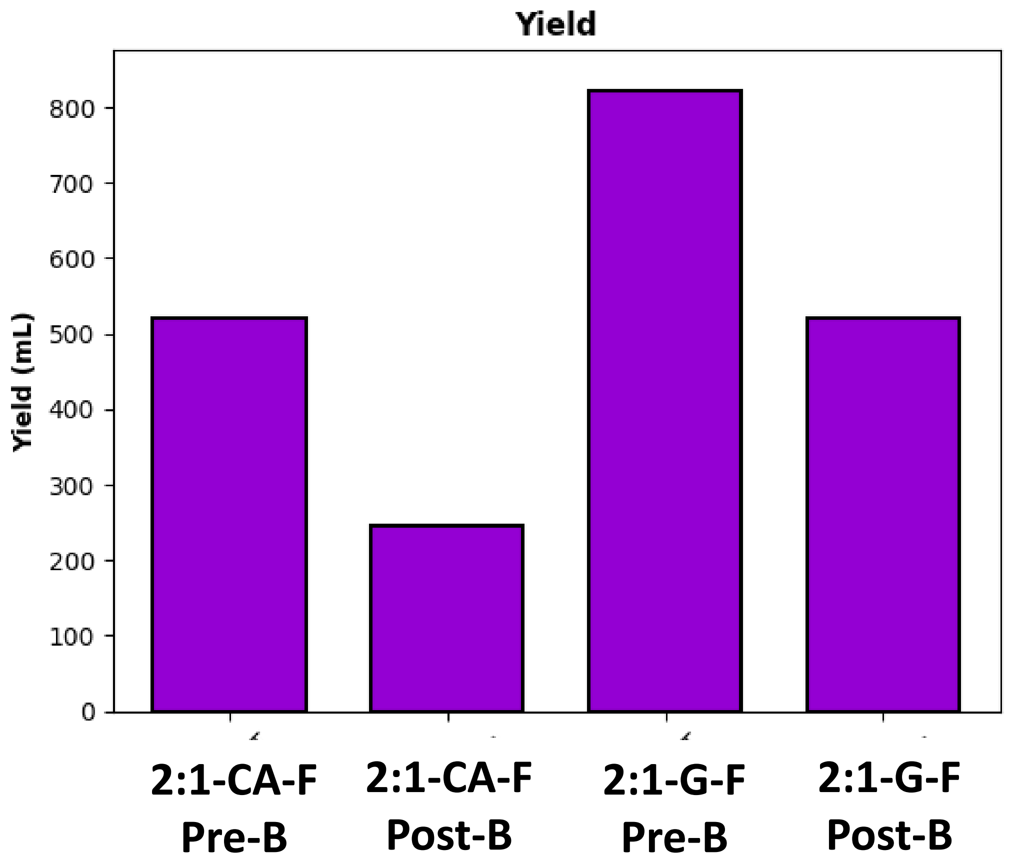

Conclusions

- **Objective 1**: Small changes in combustion synthesis parameters significantly affect material properties.
  - CA-derived catalysts with up to 10x higher specific surface area
  - G-derived catalysts had $FeAl_2O_4$-Fe_3O_4 structure, while CA-derived catalysts had γ-Fe_2O_3.
- **Objective 2**: G-derived catalysts had H_2 selectivity up to 74%, outperforming the best CA-derived catalyst by 22%.
  - The SCS fuel was the most significant synthesis parameter affecting performance.
  - Diesel dehydrogenation had better selectivity and yields versus gasoline.
- **Objective 3**: Boudouard reaction can remove both carbon residue and remove microwave-reflecting phases. *Ongoing research*.

Thank you!

Questions?

Backup slides